1 Attitude control

Content

1.1 Introduction and objectives

The 'Attitude Control Subsystem' (ACS) is in charge of the following tasks:

1) vehicle orientation during the mission,
2) vehicle stabilization about a reference attitude in presence of perturbing torques (aerodynamic, gravity gradient, solar radiation and wind, magnetic field).

The tasks are fulfilled by endowing the subsystem with suitable sensors for attitude (and rate) determination and with suitable actuators capable of exerting the necessary command torques. To this end the mass properties (position of the Centre-of-Mass, mass, moments of inertia) are essential to formulate perturbations and control torques. Important as well is the mass property variation due to propellant consumption, solar panel deployment and orientation, antennas deployment, .. One of the ACS task is to contrast the perturbation torques that would deviate the satellite from the desired attitude.

The angular momentum plays a key role in the space vehicles, since perturbations are rather small and the attitude motion is not subject to reaction torques. The previous chapters have shown that a rigid body with a null angular rate is accelerated to a non zero rate because of the external torques. If the body angular rate (spin rate) is orthogonal to the perturbing torque, a precession about the spin axis will arise. The precession rate will be proportional to the applied torque magnitude. In summary, spinning bodies behave like gyroscopes, being intrinsically resistant to external torques that are orthogonal to the spin rotation axis. The property which is referred to as gyroscopic stiffness can be employed to attenuate the effects of small and periodical perturbations.

Keeping a predefined attitude and an angular momentum implies ACS must be capable of contrasting the perturbation torques acting on the satellite, and caused by the interaction with surrounding environment. Two types of actuators are employed to the scope: (i) actuators capable of delivering external torques, as in the case of thrusters through mass ejection and magnetic torquers producing a moment of magnetic dipole that couples with the surrounding magnetic field, (ii) actuators capable of accumulating the angular momentum variations caused by the external torques, like reaction wheels and control Moment Gyros (CMG).

In addition to compensation of the environment torques, ACS must guide the operation of specific manoeuvres (slew manoeuvres) aiming to reorienting scientific instrumentation (payload), antennas, solar panels. The magnitude of the angular rate of the slew manoeuvres to be operated without interrupting the scientific mission may require separated actuation systems between pointing task and slew manoeuvres.

Actuators must be complemented with suitable sensors capable of real-time measuring the satellite attitude. A first kind of sensors determines the attitude with respect to the direction between the spacecraft and celestial bodies like Sun, Earth (infrared sensors, magnetic field) and stars. Such a sensors usually require the observation of the celestial body in a field of view. A second kind of sensors, the inertial sensors, do not require any observation instrument, but they cannot directly measure the attitude; sensors like gyroscopes measure the angular rate or equivalently the attitude increment during a time unit. Time integration of the measurements allow the attitude propagation along finite time intervals (from a minute to a few hours, depending on the sensor accuracy and the mission requirements).

Details on actuators and sensors have been provided in the specific chapter.

1.2 Control modes and requirements

1.2.1 Control modes

ACS must guarantee certain functions to the spacecraft system. Since a mission is articulated in different phases, the functions required to ACS are differ from phase to phase.

Each phase features its own kinematic, dynamic and available electric power conditions such to constrain sensor and actuator selection/design and ACS algorithms as well. As a consequence very often different sensors and actuators are employed during the different phases.

Requirements and hardware differences lead to define and implement the control modes, where each mode distinguishes because of a well defined set of sensors, actuators and control laws. Each mission phase in turn may split into different control modes.

From a rather generic standpoint, the typical ACS modes are the following.

3) Orbit insertion mode. It is employed during the phase when the spacecraft is released by the last launcher stage and enters into the nominal mission orbit. Different control options are possible, from the absence of any attitude control to the gyroscopic stabilization forced by the last rocket stage.
4) Acquisition mode. The main goal is to stabilize the spacecraft attitude, which means first to reduce the angular rates forced by the last rocket stage (rate damping) and then to bring the attitude to satisfy the electrical and thermal requirements capable of making the spacecraft autonomous. Electrical requirements include battery recharge through solar panels, switch on of telecommunication units and control devices. Thermal requirements may impose specific attitude (and rate) to allow thermal screens and radiators to orient in the expected way corresponding to the nominal temperature conditions of the on-board instruments.
5) Normal mode. It is the mode to be triggered on during the normal mission conditions. For the non scientific satellites the mode is the operating mode, which includes orbital

manoeuvres and the commissioning phase aiming to test all satellite devices and operations. For scientific satellites the normal mode is usually a preparation mode to the main mission phase; in such cases it may be referred to as Fine Pointing Mode, to enhance pointing requirements versus safety and acquisition.

6) Slew mode. During this mode the spacecraft undergoes attitude changes . Very often it is not treated as a separated mode, but as sub-mode of the normal or scientific modes.
7) Science mode. It is proper of scientific satellites and aims to satisfy the most stringent requirements in terms of accuracy.
8) Contingency or safe mode. ACS enters this mode during emergency, because of anomalies have been detected during science, slew, normal and acquisition modes. Since operations, requirements and functionalities are not very different from the acquisition mode, often it is treated as a sub-mode of the acquisition mode.

Of course each mode may split into lower level modes (sub-modes), whose transition is internal to the mode itself and thus hidden to ACS higher levels.

Each ACS mode is usually specified by

1) Input conditions: angular rates, attitude errors with respect to reference attitude.
2) Output conditions: angular rates, rate and attitude errors with respect to reference attitude.
3) Time-out: the maximum time allotted to reach the output conditions starting from the input ones.

1.2.2 Requirements

1.2.2.1 Attitude error definition

Requirements and their definition manner and procedure strongly depend on the mission and on the associated mode. In any case they include attitude and angular rate accuracy and te angular rate range within which such accuracies must be met.

It is straightforward providing an exhaustive picture of the topic, as it is still subject of discussion and regulation by the different space agencies. In the following the key definition of attitude and angular rate accuracy is given following the “ESA pointing error handbook”, that the reader is referred to for further details [10].

As defined in Chapter 1, given the ‘true’ or ‘actual’ body frame $\mathcal{R}_b$ and a ‘target’ or ‘reference’ body frame $\mathcal{R}_t$, the error between them is defined as an error rotation aligning one frame to another. In [10] the error rotation aligns the target to the body frame. Here we justify the opposite definition. To be generic, the body frame can be replaced by other frames and we adopt a generic notation dropping the subscript b, not to be restrict to body frames. Thus we distinguish between the reference frame $\underline{\mathcal{R}}$ and the ‘actual’ frame $\mathcal{R}$.

Definition 1. The error between the target frame $\underline{\mathcal{R}}$ and the 'true' $\mathcal{R}$ (or attitude error), is the rotation matrix $\underline{E} = R_t^b = \left(R_b^i\right)^T R_t^i$ that aligns $\mathcal{R}_b$ to $\mathcal{R}_t$, or transforms target coordinates into body coordinates. In other terms $\underline{E}$ is the attitude of the target frame in the body frame.

Justification comes from the usual definition of the control error as the difference between reference and actual variables. Indeed expanding $\underline{E}$ up to the 1st order term under the assumption of small angles one obtains

$$\begin{aligned} &\underline{E} = \left(R_b^i\right)^T R_t^i \cong I + \delta\underline{E} = I + \underline{\delta\boldsymbol{\theta}}\times \\ &\delta\underline{E} = \left(R_b^i\right)^T \left(R_t^i - R_b^i\right) \quad , \\ &\underline{\delta\boldsymbol{\theta}} = \begin{bmatrix} \underline{\delta\theta}_1 \\ \underline{\delta\theta}_2 \\ \underline{\delta\theta}_3 \end{bmatrix} \end{aligned} \tag{5.1}$$

where the difference between target and body attitude matrices justifies the definition. A similar result comes from employing quaternions $\boldsymbol{q}$ and $\underline{\boldsymbol{q}} = \boldsymbol{q}_t$, and holds

$$\begin{aligned} &\underline{\delta\boldsymbol{q}} = \boldsymbol{q}^{-1} \otimes \underline{\boldsymbol{q}} \cong \begin{bmatrix} 1 \\ \underline{\delta\mathbf{q}} \end{bmatrix} \cong \begin{bmatrix} 1 \\ \underline{\delta\boldsymbol{\theta}}/2 \end{bmatrix} \\ &\begin{bmatrix} q_0 & \mathbf{q}^T \\ -\mathbf{q} & q_0 I - \mathbf{q}\times \end{bmatrix} \begin{bmatrix} \underline{q}_0 \\ \underline{\mathbf{q}} \end{bmatrix} = \begin{bmatrix} q_{b0}q_{t0} + \mathbf{q}_b^T\mathbf{q}_t \cong 1 \\ q_0 q_{t0}\left(\mathbf{q}_t / q_{t0} - \mathbf{q}_b / q_{b0}\right) - \mathbf{q}_b \times \mathbf{q}_t \end{bmatrix}, \end{aligned} \tag{5.2}$$

where again the difference 'target minus body' stems.

Under the small angle assumption the following attitude sub-cases can be defined:

1) The frame error is the attitude error between two frames as defined by (5.1) and (5.2), and is represented by the 3D vector $\underline{\delta\boldsymbol{\theta}}$.
2) The misalignment of the body axis k is defined by the column $\underline{\mathbf{e}}_k$ of the matrix

$$\underline{E} = I + \underline{\delta\boldsymbol{\theta}}\times = \left[\underline{\mathbf{e}}_1 \quad \underline{\mathbf{e}}_2 \quad \underline{\mathbf{e}}_3\right]. \tag{5.3}$$

   It can be represented by the pair of Euler angles $\underline{\delta\theta}_i$ and $\underline{\delta\theta}_j$, $i, j \neq k$ in the column $\underline{\mathbf{e}}_k$ and by the cone aperture around the axis $\underline{\mathbf{e}}_k$

$$\underline{\delta\theta}_{ij} = \sqrt{\underline{\delta\theta}_i^2 + \underline{\delta\theta}_j^2}\ . \tag{5.4}$$

3) The planar misalignment of a pair of axes i, j around the axis k, defined by the error $\underline{\delta\theta}_k$.

1.2.2.2 Attitude model and prediction error

The attitude error definition (5.1) can be applied to the error between measured and 'model' quaternions, denoted by $\boldsymbol{y}$ and $\boldsymbol{q}$, respectively. The model error is defined as the error quaternion $\delta\boldsymbol{q}$ aligning model to measure, as in (5.2), i.e.

$$\boldsymbol{y} = \boldsymbol{q} \otimes \delta\boldsymbol{q} . \tag{5.5}$$

Using rotation matrices, (5.5) becomes

$$Y(\boldsymbol{y}) = R(\boldsymbol{q}) E(\delta\boldsymbol{q}) . \tag{5.6}$$

The model quaternion $\boldsymbol{q}$ is defined by the spacecraft design model, and corresponds to the 'true' quaternion $\boldsymbol{q}$ in *equation reference goes here*

1.2.2.3 Performance

The small angle assumption in (5.1) and (5.2) shows the attitude error is a vector $\delta\underline{\boldsymbol{\theta}}$ of three Euler angles (free of ordering) rotating the body frame into the target frame. Since the error angles are time functions, some norm must be adopted to assess their performance. A formal way is to assume $\delta\underline{\boldsymbol{\theta}}$ a Gaussian (zero-mean) stationary stochastic process having spectral density matrix $S^2_{\delta\underline{\theta}}(f)$ with components

$$S^2_{\delta\underline{\theta}}(f) = \begin{bmatrix} S^2_{\delta\underline{\theta}1} & S_{\delta\underline{\theta},12} & S_{\delta\underline{\theta},13} \\ S_{\delta\underline{\theta},12} & S^2_{\delta\underline{\theta},2} & S_{\delta\underline{\theta},23} \\ S_{\delta\underline{\theta},13} & S_{\delta\underline{\theta},23} & S^2_{\delta\underline{\theta},3} \end{bmatrix} (f) . \tag{5.7}$$

Performance may defined by fixing a bound to (5.7)

$$S^2_{\delta\underline{\theta}}(f) \le S^2_{\delta\underline{\theta},\max}(f) \tag{5.8}$$

over all or part of the frequency domain $f \ge 0$. Since any control variable is discrete-time, spectral density is defined up to the Nyquist frequency $f_{\max} = 0.5/T$, where T is the sampling time.

The covariance matrix $R^2_{\delta\underline{\theta}}$ is obtained by integrating (5.7) in the frequency domain

$$R^2_{\delta\underline{\theta}} = \int_0^{f_{\max}} S^2_{\delta\underline{\theta}}(f) df = \begin{bmatrix} \sigma^2_{\delta\underline{\theta},1} & \sigma_{\delta\underline{\theta},12} & \sigma_{\delta\underline{\theta},13} \\ \sigma_{\delta\underline{\theta},12} & \sigma^2_{\delta\underline{\theta},2} & \sigma_{\delta\underline{\theta},23} \\ \sigma_{\delta\underline{\theta},13} & \sigma_{\delta\underline{\theta},23} & \sigma^2_{\delta\underline{\theta},3} \end{bmatrix} , \tag{5.9}$$

where $S^2_{\delta\underline{\theta}}(f)$ has been assumed unilateral, i.e. defined for positive frequencies. Requirements are usually expressed in terms of the covariance matrix (5.9), and very often only in terms of the component variances $\sigma^2_{\delta\underline{\theta},k}$, $k = 1,2,3$. Since Gaussian random variables are not bounded, but they may assume any real value, a finite occurrence range, indicated as nσ range, is defined around the zero mean value as

$$\left|\underline{\delta\theta}_k\right| \le n\sigma_{\underline{\delta\theta},k}\,, \tag{5.10}$$

where usually $n = 3$. One must be aware that a finite probability of outliers (or extreme values) exists, although decreasing as $n \to \infty$, such that

$$P_n\left\{\underline{\delta\theta}_k\right\} = \lim_{n\to\infty} P\left\{\left|\underline{\delta\theta}_k\right| > n\sigma_{\underline{\delta\theta},k}\right\}. \tag{5.11}$$

The outlier (or extreme) probability for $n = 3$ holds $P_{n=3}\left\{\underline{\delta\theta}_k\right\} \cong 0.0027$ (see Figure 1 where $n = x/\sigma$).

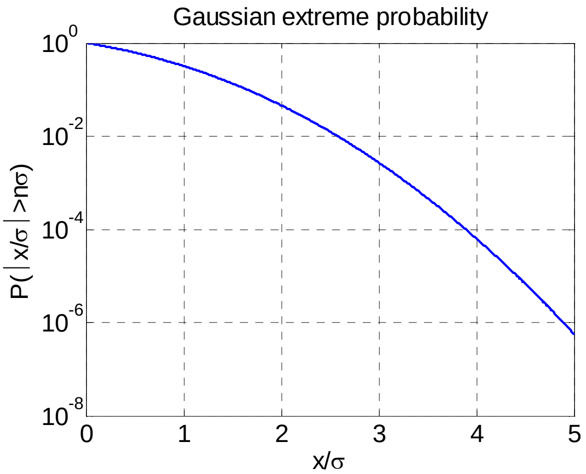

Figure 1. Gaussian extreme probability defined in (5.11).

Variance is explicitly related to (unilateral) spectral density when the stochastic process is close to be white, i.e. the spectral density $S^2_{\underline{\delta\theta},k}$ is constant (flat) for $0 \le f < f_{\max}$. In that case the variance root square (or standard deviation, or dispersion) holds

$$\sigma_{\underline{\delta\theta},k} = S_{\underline{\delta\theta},k}\sqrt{f_{\max}}\,. \tag{5.12}$$

When the spectral density is bounded but not constant and decreases from lower to higher frequencies, the simplest bound to the decreasing mid spectral density assumes a random drift takes place i.e.

$$S^2_{\underline{\delta\theta},k}\left(f\right) \le S^2_{\delta\theta,k}\left(f_0\right)\left(\frac{f_0}{f}\right)^2,\ f_0 \le f < f_1, \tag{5.13}$$

which implies that the error is strongly correlated with past and future, and it may undergo significant, though bounded, fluctuations. In the time domain, correlation implies the error equals the integral of some stochastic process

$$\underline{\delta\theta}_k(t) = \underline{\delta\theta}_k(t_0) + \int_{t_0}^{t} \underline{\delta\omega}_k(\tau) d\tau\,, \tag{5.14}$$

that in the case of the bound (5.13) has 'flat' spectral density $S^2_{\underline{\delta\omega}}(f) = S^2_{\underline{\delta\theta},k}(f_0)(2\pi f_0)^2$. In that case 'stability' conditions are required so as to limit the error fluctuations in a given time interval, i.e.

$$\left|\underline{\delta\theta}_k(t_1) - \underline{\delta\theta}_k(t_0)\right| \leq n\sigma_{\underline{\delta\theta,k}}(t_0, t_1). \tag{5.15}$$

In the case of the bound (5.13) it holds

$$\sigma_{\underline{\delta\theta},k}(t_0, t_1) = S_{\underline{\delta\theta},k}(f_0) 2\pi f_0 \sqrt{t_1 - t_0}\,. \tag{5.16}$$

The attitude error $\underline{\delta\boldsymbol{\theta}}$ is called the absolute pointing error (APE) and (5.10) is the bound inequality. The error increment $\underline{\delta\boldsymbol{\theta}}(t_1) - \underline{\delta\boldsymbol{\theta}}(t_0)$ is called the relative pointing error (RPE) and (5.15) is the bound inequality.

Exercise 1. Assuming a sampling time $T = 0.1\ \mathrm{s}$, and an APE bound of 5 arcmin (3σ) of the x-axis misalignment, $k = 1$, find the attitude error spectral density bound assuming flat density and equal apportionment between the error components, that are assumed to be statistically independent.

Solution. Using (5.12) and (5.4), and the conversion $5\ \mathrm{arcmin} \cong 1.5\ \mathrm{mrad}$, the (unilateral) density of each error component holds

$$S_{\underline{\delta\theta},2}(f) = S_{\underline{\delta\theta},2}(f) = \frac{1.5\times10^{-3}}{3\sqrt{2}\sqrt{5}} \cong 0.15\ \frac{\mathrm{mrad}}{\sqrt{\mathrm{Hz}}}. \tag{5.17}$$

Similar definitions and bound inequalities refer to the angular rate error

1.3 Passive and active control

The ACS objectives can be summarized into (i) vehicle attitude stabilization about a reference attitude and (ii) tracking of attitude manoeuvres. Attitude stabilization can be achieved either in a passive or active way; attitude manoeuvres can only be performed by an active control system.

1) Passive control achieves attitude stabilization by exploiting the interactions with the surrounding environment. Attitude dynamics and kinematics under environment perturbations (for instance the gravity gradient torques, aerodynamic torques) can establish a finite number of asymptotically stable attitude and rate equilibria. If the spacecraft attitude is capable of reaching one equilibrium point, it can be kept in absence of large perturbations (because of a nonlinear dynamics). Equilibria can be designed by giving the spacecraft appropriate mass, shape and surface properties. Thus around any equilibrium a stability region must be defined, and corrective actions should to envisaged

to recover the region in the case of large perturbations. Such actions can only be ensured by an active control, which thus is demanded to assist passive control in emergency conditions.

2) Active control is such to apply suitable and explicit torques to guide and keep attitude and angular rate close to reference values. Each attitude and angular rate (the whole state) is a candidate to be an equilibrium state, which implies that active control can both stabilize and manoeuvre the spacecraft attitude. The active control employs a mix of open-loop actions, directly imposed by the reference signals, and of closed-loop actions which are functions of the tracking errors between reference and measured attitude and rate.

1.4 Passive control

The commonest form of passive control are:

1) gyroscopic stabilization: the satellite is made rotating about the principal axis with the largest moment of inertia (single-spin satellites),
2) gravity-gradient stabilization: a space vehicle with asymmetric mass distribution tends to align the axis with the leas moment of inertia along the local vertical,
3) aerodynamic stabilization: centre of mass and centre of pressure are separated so as to create a stabilizing aerodynamic torque; separation is obtained through suitable mass distribution and aerodynamic surfaces (winglets).

1.4.1 Gyroscopic stabilization

In Chapter 2 the free response study of the attitude dynamics has shown the rotation about a principal inertia axis is an equilibrium state. In absence of power dissipation rotation about the principal axes with largest and smallest inertia is a stable equilibrium. Unavoidable power dissipation restricts stability about the axis with larges inertia. Recall the dynamic equation about the CoM from Chapter 2

$$\dot{\vec{H}}_c = \vec{M}_c , \tag{5.18}$$

where $\vec{M}_c$ is only due to perturbation torques. Integrating the equation from t_0 to t, where the interval is defined by the mission lifetime, one finds the angular momentum variation

$$\Delta\vec{H}_c\left(t,t_0\right) = \vec{H}_c\left(t\right) - \vec{H}_c\left(t_0\right) = \int_{t_0}^{t} \vec{M}_c\left(\tau\right)d\tau . \tag{5.19}$$

Considering the mean angular momentum

$$\underline{\vec{H}}_c\left(t_0,t\right) = \frac{1}{t-t_0}\int_{t_0}^{t} \vec{H}_c\left(\tau\right)d\tau , \tag{5.20}$$

the magnitude of the angular momentum variation in (5.19) must be sufficiently smaller than the mean value in (5.20)

$$\left|\Delta\vec{H}_c\left(t,t_0\right)\right| << \left|\underline{\vec{H}}_c\left(t_0,t\right)\right|. \tag{5.21}$$

The momentum variation accounts for mean angular rate (magnitude and direction) variation.

If the perturbing torques in (5.19) are short-term periodic, i.e. they are zero-mean and their periodic components are tuned to the orbit and spin periods, the integral in (5.19) can be taken as bounded, and the average angular momentum $\underline{\vec{H}}_c\left(t_0,t\right)$ can be designed to satisfy (5.21). If the torques instead contain secular terms, i.e. long terms drifts, (5.19) tends to be unbounded and (5.21) cannot be guaranteed. In that case an active control must be implemented, at least to counteract the secular components. Usually the active control is discontinuous, i.e. only intervenes when either the angular momentum or the attitude exceed the prescribed tolerance.-

The single-spin systems are very simple, but it fits only very specific missions. More complex gyro-stabilized control systems are

1) Dual-spin: the spacecraft is made by two parts rotating at different angular speeds. One part is the ‘true’ spacecraft carrying the payload, the other is a rotor which is rotating at a much higher speed.
2) Momentum bias: the spacecraft includes an inertia wheel which is rotating to provide the vehicle with a specified gyro stiffness.

1.4.2 Gravity gradient stabilization in a circular orbit

1.4.2.1 Equilibrium

Assume as before the spacecraft body frame $\mathscr{R}_b$ must be aligned with the LVLH (local) frame $\mathscr{R}_l$ defined by a circular orbit with radius $r_c = a$. Assuming perfect alignment of the body frame with the local one, the only satellite angular rate is due to the orbit itself

$$\boldsymbol{\omega} = \begin{bmatrix} 0 \\ \omega_2 = \omega_o = \sqrt{\mu_E / a^3} \\ 0 \end{bmatrix}, \tag{5.22}$$

and the CoM position in local or body coordinates holds

$$\mathbf{r}_c = \begin{bmatrix} 0 \\ 0 \\ z_c = a \end{bmatrix}. \tag{5.23}$$

To be generic the body axes are not principal, and the inertia matrix J is generic. The generic Euler equation, forced by the generic gravity gradient becomes

$$\begin{aligned} & J\begin{bmatrix} \dot{\omega}_1 \\ \dot{\omega}_2 \\ \dot{\omega}_3 \end{bmatrix} = -\begin{bmatrix} 0 & 0 & \omega_o \\ 0 & 0 & 0 \\ -\omega_o & 0 & 0 \end{bmatrix}\begin{bmatrix} J_{11} & J_{12} & J_{13} \\ J_{12} & J_{22} & J_{23} \\ J_{13} & J_{23} & J_{33} \end{bmatrix}\begin{bmatrix} 0 \\ \omega_o \\ 0 \end{bmatrix} + 3\omega_o^2\begin{bmatrix} -J_{23} \\ J_{13} \\ 0 \end{bmatrix} = \\ & = \omega_o^2\begin{bmatrix} -J_{23} \\ 0 \\ J_{12} \end{bmatrix} + 3\omega_o^2\begin{bmatrix} -J_{23} \\ J_{13} \\ 0 \end{bmatrix} \end{aligned} . \tag{5.24}$$

Looking for the angular rate equilibrium $\dot{\boldsymbol{\omega}} = 0$, the following equation is obtained

$$0 = \begin{bmatrix} -J_{23} - 3J_{23} \\ 3J_{13} \\ J_{12} \end{bmatrix}, \tag{5.25}$$

which is only satisfied if the products of inertia are zero, i.e. the principal axes are aligned with the LVLH frame. The equilibrium rate $\underline{\boldsymbol{\omega}}$ is given by (5.22).

1.4.2.2 Stability of the equilibrium

The aim is to derive conditions for the stability of the rate equilibrium (5.22) to be completed with attitude equilibrium $\underline{\boldsymbol{\theta}} = 0$. Textbooks [7] and are followed. Misalignment between local and body frame (principal axes) is accounted for by small Euler angles $\boldsymbol{\theta} = \{\varphi, \theta, \psi\}$, which implies from that the CoM position can be approximated as

$$\mathbf{r}_c = \left(R_b^l\right)^T \begin{bmatrix} 0 \\ 0 \\ r_c \end{bmatrix} \cong \begin{bmatrix} -\theta \\ \varphi \\ 1 \end{bmatrix} r_c , \tag{5.26}$$

and the gravity gradient acceleration can be restricted to linear terms in the Euler angles

$$J^{-1}\mathbf{M}_g(t) = \frac{3\mu_E}{r_c^5}\begin{bmatrix} (J_3 - J_2)y_c z_c / J_1 \\ (J_1 - J_3)x_c z_c / J_2 \\ (J_2 - J_1)x_c y_c / J_3 \end{bmatrix} \cong 3\omega_o^2 \begin{bmatrix} -\varphi\sigma_1 \\ \theta\sigma_2 \\ 0 \end{bmatrix}. \tag{5.27}$$

The state equation of the equilibrium perturbations has been derived in Section but with generic external torques. Adding the gravity-gradient acceleration (5.27) in the state equation and setting other input signals to zero, $\mathbf{u}$=0, the perturbation equation becomes

$$\dot{\mathbf{x}}(t) = A\mathbf{x}(t)$$
$$A = \left[\begin{array}{ccc|ccc} 0 & 0 & 0 & 1 & 0 & 0 \\ 0 & 0 & 0 & 0 & 1 & 0 \\ 0 & 0 & 0 & 0 & 0 & 1 \\ \hline -4\omega_o^2\sigma_1 & 0 & 0 & 0 & 0 & -\omega_o(1-\sigma_1) \\ 0 & 3\omega_o^2\sigma_2 & 0 & 0 & 0 & 0 \\ 0 & 0 & \omega_o^2\sigma_3 & \omega_o(1+\sigma_3) & 0 & 0 \end{array}\right],\ \mathbf{x} = \begin{bmatrix} \varphi \\ \theta \\ \psi \\ \hline \dot{\varphi} \\ \dot{\theta} \\ \dot{\psi} \end{bmatrix}. \tag{5.28}$$

where the coefficients σ_k in are repeated here and replaced with the coefficients μ_k which are more suitable to derive stability conditions

$$\begin{bmatrix} \sigma_1 \\ \sigma_2 \\ \sigma_3 \end{bmatrix} = \begin{bmatrix} \mu_1 \\ -\mu_2 \\ -\mu_3 \end{bmatrix} = \begin{bmatrix} (J_2 - J_3)/J_1 \\ (J_3 - J_1)/J_2 \\ (J_1 - J_2)/J_3 \end{bmatrix}. \tag{5.29}$$

Kinematics and dynamics of θ (pitch), describing the rotation about the orbit normal, is decoupled from roll and yaw. The latter are instead linked through their angular rates. To this end, equation (5.28) is rearranged in two separate equations using μ_k

$$\begin{aligned} \begin{bmatrix} \dot{\varphi} \\ \dot{\psi} \\ \ddot{\varphi} \\ \ddot{\psi} \end{bmatrix}(t) &= \begin{bmatrix} 0 & 0 & 1 & 0 \\ 0 & 0 & 0 & 1 \\ -4\omega_o^2\mu_1 & 0 & 0 & -\omega_o(1-\mu_1) \\ 0 & -\omega_o^2\mu_3 & \omega_o(1-\mu_3) & 0 \end{bmatrix} \begin{bmatrix} \varphi \\ \psi \\ \dot{\varphi} \\ \dot{\psi} \end{bmatrix}(t) \\ \begin{bmatrix} \dot{\theta} \\ \ddot{\theta} \end{bmatrix}(t) &= \begin{bmatrix} 0 & 0 \\ -3\omega_o^2\mu_2 & 0 \end{bmatrix} \begin{bmatrix} \theta \\ \dot{\theta} \end{bmatrix}(t) \end{aligned}. \tag{5.30}$$

Therefore the stability conditions can be separated in two parts.

1) Pitch stability, θ: the second equation in (5.30) and (5.29) provide the inequality

$$\mu_2 > 0 \Rightarrow J_1 > J_3, \tag{5.31}$$

which makes the eigenvalues to be imaginary and equal to

$$\lambda_\theta = \pm j\omega_o\sqrt{\mu_2}\ . \tag{5.32}$$

2) Roll and yaw stability: the characteristic polynomial of the first equation in (5.30) is

$$\lambda^4 + (1 + 3\mu_1 + \mu_1\mu_3)\omega_o^2\lambda^2 + 4\omega_o^4\mu_1\mu_3 = \lambda^4 + a\omega_o^2\lambda^2 + b\omega_o^4\,. \tag{5.33}$$

Stability conditions corresponding to pure imaginary roots, can be derived from the inspection of the polynomial roots

$$\lambda = \pm\omega_o\sqrt{-\frac{1}{2}\left(a \pm \sqrt{a^2 - 4b}\right)}, \tag{5.34}$$

leading to the necessary and sufficient conditions

$$\begin{aligned} & b = 4\mu_1\mu_3 > 0 \\ & a = 1 + 3\mu_1 + \mu_1\mu_3 > 2\sqrt{\mu_1\mu_3} \end{aligned}. \tag{5.35}$$

Combining inequality (5.31) with the former in (5.35), restricted to $\mu_1 > 0,\ \mu_3 > 0$ (sufficient condition) provides

$$J_1 > J_3,\ J_2 > J_1,\ J_2 > J_3 \tag{5.36}$$

which latter restricts to the alternative inequalities, referred to as Lagrange inequalities

$$\begin{aligned} & J_2 > J_1 > J_3 \\ & \mu_1 > \mu_3 > 0 \end{aligned}. \tag{5.37}$$

It may be represented graphically by noticing that $|\mu_1| \le 1$ and $|\mu_3| \le 1$

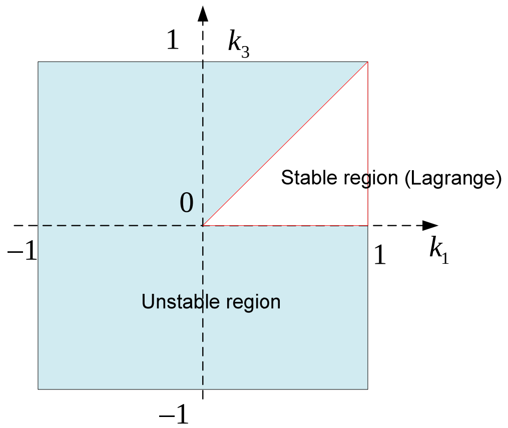

Figure 2. Unstable and stable regions.

To understand how to simply implement a spacecraft satisfying (5.37) consider a main spherical body of radius r with equal moments of inertia J and three perpendicular rods of mass $m_k = 2\mu l_k$, $k = 1, 2, 3$, half-length $l_k > r$, and density μ per unit of length symmetrically projecting out of the main body The moment of inertia of a long slender rod around its CoM holds $J_k = 2m_k l_k^2/3 = 4\mu l_k^3/3$, which leads to

$$
\begin{aligned}
J_1 &= J + \frac{4}{3}\mu\left(l_3^3 + l_2^3\right) \\
J_2 &= J + \frac{4}{3}\mu\left(l_3^3 + l_1^3\right). \\
J_3 &= J + \frac{4}{3}\mu\left(l_1^3 + l_2^3\right)
\end{aligned}
\tag{5.38}
$$

Inequality (5.37) implies the reverse inequality, namely

$$l_3 > l_1 > l_2 \,. \tag{5.39}$$

Of course the rods (usually called ‘booms’) cannot be made of arbitrary length, as they must be stored inside the main body during launch, and vibrations must be prevented as well. It was a common passive stabilization during early epoch of space missions. As an example the Soviet Union’s Salyut-6/Soyuz space station (1977-1982) in Figure 3 spent much of its time in a gravity-gradient stabilized mode. The station orientation in Figure 3 satisfies (5.37).

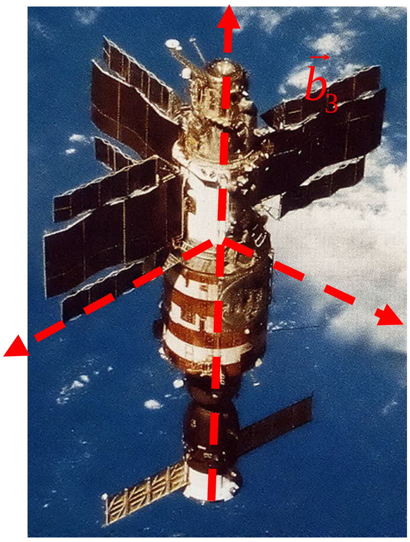

Figure 3. The Soviet space station Salyut 7 seen from the manned spacecraft Soyuz-T13 after undocking in 1985.

Remarks. Conditions (5.31) and (5.35) are necessary and sufficient for infinitesimal stability, i.e. under arbitrary small perturbations around the equilibrium point. Actually Lagrange region can be shown via Lyapunov function to be stable in the large. A further problem are conditions for asymptotical stability which requires some energy loss on the spacecraft.

Remarks. Gravity-gradient effects were first studied by D’Alembert and Euler in 1749. Later in 1780, Lagrange used it to explain why the Moon always has the same face toward the Earth. Indeed the Moon is slightly elongated in the direction pointing to the Earth.

1.4.2.3 <u>Aerodynamic stability of a boxlike spacecraft under small attitude</u>

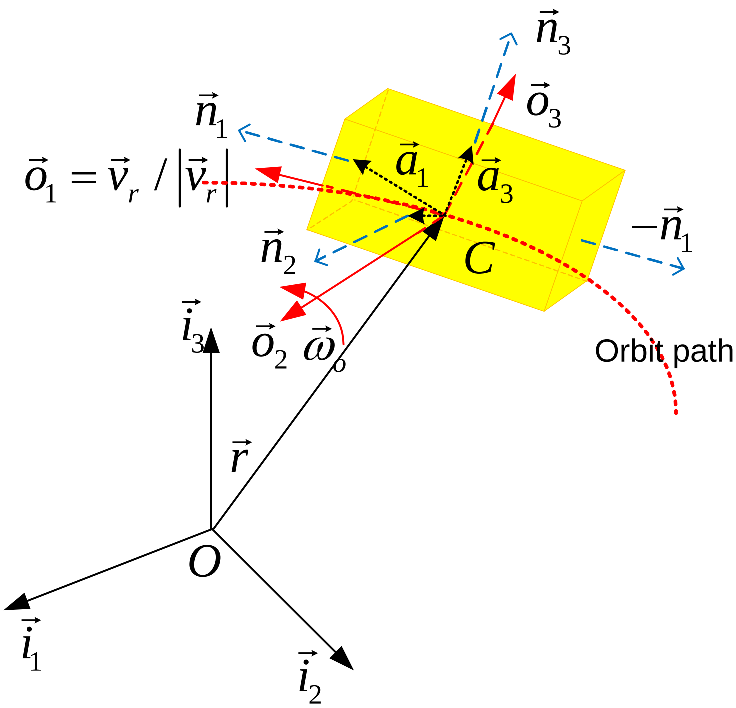

Figure 4. Boxlike spacecraft.

Consider a boxlike spacecraft in Figure 4 having $n = 6$ surfaces with the same drag coefficient C_D, that are grouped in pairs $k = 1,2,3$, each pair (front, lateral and top) having the same area A_k and opposite normal vectors $\vec{n}_k$. The body coordinates of the latter are

$$\mathbf{n}_1 = \begin{bmatrix} s_1 = \pm 1 \\ 0 \\ 0 \end{bmatrix}, \ \mathbf{n}_2 = \begin{bmatrix} 0 \\ s_2 = \pm 1 \\ 0 \end{bmatrix}, \ \mathbf{n}_3 = \begin{bmatrix} 0 \\ 0 \\ s_3 = \pm 1 \end{bmatrix}, \tag{5.40}$$

where s_k refers to positive and negative surface. Assume also the CoP to be symmetric for each pair, i.e. in body coordinates

$$\mathbf{a}_1 = \begin{bmatrix} s_1 a_{11} \\ a_{12} \\ a_{13} \end{bmatrix}, \mathbf{a}_1 = \begin{bmatrix} a_{21} \\ s_2 a_{22} \\ a_{23} \end{bmatrix}, \mathbf{a}_3 = \begin{bmatrix} a_{31} \\ a_{32} \\ s_3 a_{33} \end{bmatrix}, \tag{5.41}$$
$$a_{11} > 0, a_{22} > 0, a_{33} > 0$$

If the satellite moves in a quasi-circular orbit, and the first axis of the Local Orbital Frame $\mathscr{R}_o = \{C, \vec{o}_1, \vec{o}_2, \vec{o}_3\}$ defined in Chapter 1 to be oriented as the relative speed vector: $\vec{o}_1 = \vec{e}_v$. Let the attitude $\boldsymbol{\theta}$ of the body frame $\mathscr{R}_b = \{C, \vec{b}_1, \vec{b}_2, \vec{b}_3\}$ be defined with sequence 3-2-1. Applying the 3-2-1 body-to-fixed transformation $R_b^o = R_b^e$ defined in Chapter 1 to the orbital frame, the body coordinates of $\vec{o}_1 = \vec{e}_v$ hold and are approximated in the case of small angles as

$$\mathbf{e}_v = \left(R_b^o\right)^T \begin{bmatrix} 1 \\ 0 \\ 0 \end{bmatrix} = \begin{bmatrix} c_\theta c_\psi \\ s_\varphi s_\theta c_\psi - s_\psi c_\varphi \\ c_\varphi s_\theta c_\psi + s_\psi s_\varphi \end{bmatrix} \cong \begin{bmatrix} 1 \\ -\psi \\ \theta \end{bmatrix}. \tag{5.42}$$

Compute now the three angular factors in, under small Euler angles, which rules out the back surface defined by $s_1 = -1$

$$\begin{aligned} &\max\left(\cos\alpha_1, 0\right) = 1 \\ &\max\left(\cos\alpha_2, 0\right) = -s_2\psi , \\ &\max\left(\cos\alpha_3, 0\right) = s_3\theta \end{aligned} \tag{5.43}$$

and the cross products

$$\mathbf{a}_1 \times \mathbf{e}_v = \begin{bmatrix} a_{13}\psi + a_{12}\theta \\ a_{13} - a_{11}\theta \\ -a_{12} - a_{11}\psi \end{bmatrix}, \mathbf{a}_2 \times \mathbf{e}_v = \begin{bmatrix} 0 \\ a_{23} \\ -s_2 a_{22} \end{bmatrix}, \mathbf{a}_3 \times \mathbf{e}_v = \begin{bmatrix} 0 \\ s_3 a_{33} \\ -a_{32} \end{bmatrix}, \tag{5.44}$$

where 2nd order terms have been dropped. The drag torque vector is found to be

$$\begin{aligned} &\mathbf{M}_D \cong -p_a C_D \begin{bmatrix} A_1\left(a_{13}\psi + a_{12}\theta\right) \\ A_1\left(a_{13} - a_{11}\theta\right) - s_2\psi A_2 a_{23} + \theta A_3 a_{33} \\ -A_1\left(a_{12} + a_{11}\psi\right) + \psi A_2 a_{22} - s_3\theta A_3 a_{32} \end{bmatrix}. \\ &p_a = \frac{1}{2}\rho v_r^2 \end{aligned} \tag{5.45}$$

The expression (5.45) can be made free of sign by noticing that $s_2\psi < 0$, and $s_3\theta > 0$, which leads to

$$\mathbf{M}_D \cong -p_a C_D \begin{bmatrix} A_1\left(a_{13}\psi + a_{12}\theta\right) \\ A_1\left(a_{13} - a_{11}\theta\right) + |\psi| A_2 a_{23} + \theta A_3 a_{33} \\ -A_1\left(a_{12} + a_{11}\psi\right) + \psi A_2 a_{22} - |\theta| A_3 a_{32} \end{bmatrix}. \tag{5.46}$$

A symmetrical design imposes the CoP of the surface $k = 1$ to lie on the body axis, i.e.

$$a_{12} = a_{13} = 0. \tag{5.47}$$

Further imposing the lateral and top/bottom surfaces to be symmetrical with respect to their normal axis yields

$$a_{23} = a_{32} = 0. \tag{5.48}$$

Thus (5.46) simplifies to

$$\mathbf{M}_D \cong -p_a C_D A_1 \begin{bmatrix} 0 \\ \left(-a_{11} + A_3 a_{33} / A_1\right)\theta \\ \left(-a_{11} + A_2 a_{22} / A_1\right)\psi \end{bmatrix} = -F_D \begin{bmatrix} 0 \\ \lambda_3 \theta \\ \lambda_2 \psi \end{bmatrix}. \quad (5.49)$$

Consider the kinematics and dynamics about the orbit frame in, and restrict to the second Euler angle θ_2 (pitch) about the orbit normal $\vec{o}_2$ in Figure 4. Adding the drag torque in (5.49) and the gravity gradient in (5.25), the second order equation is obtained

$$\begin{bmatrix} \dot{\theta} \\ \ddot{\theta} \end{bmatrix}(t) = \begin{bmatrix} 0 & 1 \\ 3\omega_o^2\left(J_3 - J_1\right)/J_2 - F_D\lambda_3/J_2 & 0 \end{bmatrix} \begin{bmatrix} \theta \\ \dot{\theta} \end{bmatrix}(t), \ \begin{bmatrix} \theta \\ \dot{\theta} \end{bmatrix}(0) = \begin{bmatrix} \theta_0 \\ \dot{\theta}_0 \end{bmatrix}. \quad (5.50)$$

Stability condition immediately holds

$$\lambda_3 = -a_{11} + A_3 a_{33} / A_1 > \frac{3\omega_O^2}{F_D}\left(J_3 - J_1\right). \quad (5.51)$$

To be generic assume the spacecraft CoM not be centered on the axis $\vec{b}_1$, which implies the first coordinate a_{11} of $\vec{a}_1$ (front surface) to be different from the half axial length L. The surface areas A_k, together with λ_2 and λ_3 can now be computed as

$$\begin{aligned} A_1 &= 4a_{22}a_{33} \\ A_2 &= 4La_{33} \\ A_3 &= 4La_{22} \\ \lambda_3 &= \lambda_2 = L - a_{11} \end{aligned}, \quad (5.52)$$

Then the stability condition (5.51) becomes

$$\lambda_3 = \lambda_3 = L - a_{11} > \frac{3\omega_o^2}{F_D}\left(J_3 - J_1\right), \quad (5.53)$$

which implies the CoM must be shifted ahead of the CoP. The shift when small compared to the spacecraft length $2L$, may be achieved by placing more mass ahead or protruding a boom (thin rod) from the front surface. The design should account for uncertainty in the atmosphere density and mass variation due to propellant consumption.

Exercise 2. Consider the parameters in of the GOCE satellite () together with $L = 2.6$ m and $F_D = 8$ mN, providing

$$L - a_{11} > \frac{3\omega_o^2}{F_D}\left(J_3 - J_1\right) \cong 1.28 \text{ m}, \quad (5.54)$$

a shift that cannot be implemented. Therefore zero attitude is unstable for GOCE, and must be actively stabilized. In the GOCE case aerodynamic stability has been achieved with suitable extra surfaces which can only only guarantee stability far from the zero attitude.

1.4.2.4 Aerodynamic stability in the large

Aerodynamic stabilization may be achieved about non zero attitude, i.e. by considering large Euler angles. To simplify the formulation assume

1) the CoP of the front/back surface is along the normal, which implies $a_{12} = a_{13} = 0$,
2) $a_{23} = a_{32} = 0$
3) roll φ and yaw ψ are assumed small,
4) only pitch stability in the large condition will be looked for, i.e.

$$\underline{\varphi} = 0, \left|\underline{\theta}\right| < \pi / 2, \underline{\psi} = 0 . \tag{5.55}$$

The following CoP and nominal velocity direction result

$$\begin{aligned} & \mathbf{a}_1 = \begin{bmatrix} s_1 a_{11} \\ 0 \\ 0 \end{bmatrix}, \mathbf{a}_1 = \begin{bmatrix} a_{21} \\ s_2 a_{22} \\ 0 \end{bmatrix}, \mathbf{a}_3 = \begin{bmatrix} a_{31} \\ 0 \\ s_3 a_{33} \end{bmatrix}, \ \mathbf{e}_v = \begin{bmatrix} c_\theta \\ 0 \\ s_\theta \end{bmatrix}. \\ & a_{11} > 0, a_{22} > 0, a_{33} > 0 \end{aligned} \tag{5.56}$$

Following the same steps as in the previous section, we define the trigonometric quantities

$$\begin{aligned} & \max\left(\cos\alpha_1, 0\right) = s_1 c_\theta \geq 0 \\ & \max\left(\cos\alpha_2, 0\right) = 0 \qquad , \\ & \max\left(\cos\alpha_3, 0\right) = s_3 s_\theta = \left|s_\theta\right| \geq 0 \end{aligned} \tag{5.57}$$

and the torque directions

$$\mathbf{a}_1 \times \mathbf{e}_v = \begin{bmatrix} 0 \\ -s_1 a_{11} s_\theta \\ 0 \end{bmatrix}, \mathbf{a}_2 \times \mathbf{e}_v = \begin{bmatrix} s_2 a_{22} s_\theta \\ -a_{21} s_\theta \\ -s_2 a_{22} c_\theta \end{bmatrix}, \mathbf{a}_3 \times \mathbf{e}_v = \begin{bmatrix} 0 \\ s_3 a_{33} c_\theta - a_{31} s_\theta \\ 0 \end{bmatrix}, \tag{5.58}$$

Finally combining (5.57) and (5.58)

$$\begin{aligned}\mathbf{M}_D &\cong -p_a C_D \begin{bmatrix} 0 \\ \left(\left(-A_1 a_{11} + A_3 a_{33}\right) c_\theta - A_3 a_{31} s_3 s_\theta\right) s_\theta \\ 0 \end{bmatrix} = \\ &= -p_a C_D \begin{bmatrix} 0 \\ \left(\left(-A_1 a_{11} + A_3 a_{33}\right) c_\theta - A_3 a_{31} \left|s_\theta\right|\right) s_\theta \\ 0 \end{bmatrix}\end{aligned}. \tag{5.59}$$

The expression in (5.59) shows that only front and back surfaces $k = 1$ and the top ones contribute to pitch component.

Assuming the body axes are principal and rewriting the gravity-gradient torque from under the previous assumptions we found that

$$\mathbf{M}_g\left(t\right) = \frac{3}{2}\omega_o^2 \begin{bmatrix} 0 \\ -\left(J_1 - J_3\right) s_{2\theta} \\ 0 \end{bmatrix},\ \omega_o^2 = \frac{\mu_E}{a^3}. \tag{5.60}$$

Consider the 3-2-1 attitude kinematics from Chapter 1 and Section under zero roll and yaw, which provides

$$\begin{bmatrix} \dot\varphi \\ \dot\theta \\ \dot\psi \end{bmatrix}\left(t\right) = \begin{bmatrix} 1 & 0 & \tan\theta \\ 0 & 1 & -\varphi \\ 0 & 0 & 1/\cos\theta \end{bmatrix} \begin{bmatrix} \omega_1 \\ \omega_2 \\ \omega_3 \end{bmatrix}\left(t\right) - \omega_o \begin{bmatrix} 0 \\ 1 \\ 0 \end{bmatrix}. \tag{5.61}$$

and assume to find pitch equilibria in the range $\left|\theta\right| < \pi/2$ to avoid gimbal lock. Inserting (5.59) and (5.60) in the Euler's dynamics and looking for the equilibrium under (5.63) we obtain

$$\begin{aligned} &J\dot{\boldsymbol{\omega}}\left(t\right) = J\Omega\left(\boldsymbol{\omega}\right)\boldsymbol{\omega}\left(t\right) + \underline{\mathbf{M}}_D\left(t\right) + \underline{\mathbf{M}}_g\left(t\right) \\ &\begin{bmatrix} J_1\dot\omega_1 \\ J_2\dot\omega_2 \\ J_3\dot\omega_3 \end{bmatrix}\left(t\right) = \begin{bmatrix} \omega_2\omega_3\left(J_2 - J_3\right) \\ \omega_1\omega_3\left(J_3 - J_1\right) \\ \omega_1\omega_2\left(J_1 - J_2\right) \end{bmatrix} + \frac{3}{2}\omega_o^2 \begin{bmatrix} 0 \\ \left(J_3 - J_1\right) s_{2\theta} \\ 0 \end{bmatrix} - . \\ &-p_a C_D \begin{bmatrix} 0 \\ \left(\left(-A_1 a_{11} + A_3 a_{33}\right) c_\theta - A_3 a_{31} \left|s_\theta\right|\right) s_\theta \\ 0 \end{bmatrix} \end{aligned} \tag{5.62}$$

Equation (5.62) can be adapted to the case in which the top/bottom surfaces are split into

1) top/bottom surfaces of area A_3 that are symmetric with respect to the CoM along $\vec{b}_1$, i.e. with $a_{31} = 0$;

2) surfaces of area A_{3t} placed at $a_{33}=0$, but displaced along $\vec{b}_1$, i.e. with $a_{31}\neq 0$, thus acting as fins.

Solving equations (5.61) and (5.62) at equilibrium and splitting the top/bottom surfaces as before we find

$$\underline{\boldsymbol{\omega}}=\begin{bmatrix}0\\ \omega_o\\ 0\end{bmatrix},\qquad (5.63)$$

$$\operatorname{sgn}(\underline{\theta})\tan\underline{\theta}=-\frac{3\omega_o^2(J_3-J_1)}{p_aC_DA_{3t}a_{31}}-\frac{A_1a_{11}-A_3a_{33}}{A_{3t}a_{31}},\ \underline{\theta}=0$$

where three pitch equilbria are found. Finally assuming $\left|A_1a_{11}-A_3a_{33}\right|<<3\omega_o^2(J_3-J_1)/(p_aC_D)$, $C_D\cong 2$, $|v_r|=\omega_o(R_E+h)$, the simplified pitch equilibrium results

$$\underline{\theta}=\pm\tan^{-1}\left(-\frac{3\omega_o^2(J_3-J_1)}{p_aC_DA_{3t}a_{31}}\right)\cong\pm\tan^{-1}\left(-\frac{3(J_3-J_1)}{\rho(R_E+h)^2A_{3t}a_{31}}\right),\ \underline{\theta}=0,\qquad (5.64)$$

where $A_{3t}a_{31}$ can be adjusted to obtain the desired equilibrium. For instance given the atmosphere density $\rho\cong 0.1\times 10^{-9}\ \text{kg/m}^3$ at about $h=300\ \text{km}$, $J_3-J_1\cong 2500\ \text{kgm}^2$, $R_E\cong 6378\ \text{km}$, and the desired equilibrium $\underline{\theta}=\pm\pi/4$

$$A_{3t}a_{31}=\pm 1.85\ \text{m}^3,\ A_{3t}\geq 0,\qquad (5.65)$$

where $|a_{31}|\leq L/2$, L being the spacecraft length along $\vec{b}_1$. Thus the equilibrium pitch may be made closer to zero by increasing A_{3t}.

The pitch equilibrium stability is studied on the single-degree of freedom equation from (5.61) and (5.62)

$$\begin{aligned}&\dot{\theta}(t)=\omega_2-\omega_o-\varphi\omega_3\\ &J_2\dot{\omega}_2\cong\omega_1\omega_3(J_3-J_1)+\left(3\omega_o^2(J_3-J_1)c_\theta+p_aC_DA_{3t}a_{31}|s_\theta|\right)s_\theta\end{aligned}.\qquad (5.66)$$

Expansion about the pitch equilibrium provides

$$\begin{aligned}&\delta\dot{\theta}(t)=\delta\omega_2\\ &J_2\delta\dot{\omega}_2=\left(3\omega_o^2(J_3-J_1)\cos(2\underline{\theta})+2p_aC_DA_{3t}a_{31}\cos\underline{\theta}|\sin\underline{\theta}|\right)\delta\theta\end{aligned},\qquad (5.67)$$

and the stability condition

$$A_{3t}a_{31}<-\frac{3\omega_o^2(J_3-J_1)\cos(2\underline{\theta})}{2p_aC_D\cos\underline{\theta}|\sin\underline{\theta}|},\ |\underline{\theta}|<\pi/2.\qquad (5.68)$$

Restricting to the case $J_3 > J_1$ (slim spacecraft) like GOCE in

1) the zero pitch case is unstable,
2) the non zero pitch case $0 < |\underline{\theta}| \le \pi/4$ corresponding to $\cos(2\underline{\theta}) \ge 0$ is stable for $A_{3t}a_{31} < 0$, which implies the fins must be mounted on the spacecraft tail, $a_{31} < 0$;
3) the non zero pitch case $\pi/4 < |\underline{\theta}| < \pi/2$ corresponding to $\cos(2\underline{\theta}) < 0$ is stable also for some $A_{3t}a_{31} > 0$.

1.5 Architecture of an active attitude control system

An active attitude control system, but the same architecture applies to other active control systems, consists of:

1) sensors that are necessary to compute the errors feeding the closed loop command, they were treated in Chapter 4,
2) actuators applying the command to the spacecraft, they were treated in Chapter 4,
3) control processor or control unit or controller, in charge of computing the control algorithms, control processors are outside the textbook goal. They are numerical processors with suitable interfaces toward on-board devices, like sensors and actuators. The computing capacity in MIPS, MFLOPS, and the computing resources like the RAM memory, used in the space-bound computers are rather inferior to the same capacities on a Personal Computer. This is due to the space harsh environment (especially radiations) and to the very limited on-board power.

The higher level (essential) architecture of the control unit of an ACS is outlined in Figure 5. The three functions there reported are in charge of the standard tasks. The phase sequencer can be hidden in the reference generator. Fault detection, isolation and recovery (FDIR) is partly subdivided between the state predictor and the reference generator, but it will not detailed here. Continuous time t is used in Figure 5, but signals are exchanged at discrete-times t_i, $i = 0,1,\ldots$.

1) The reference generator (also attitude guidance) is in charge of computing the desired attitude (quaternion $\underline{\mathfrak{q}}$), angular rate $\underline{\boldsymbol{\omega}}$ and acceleration $\underline{\mathbf{a}}_q = \dot{\underline{\boldsymbol{\omega}}}$ for each mission phase. To this end it must be capable of switching between one phase to another with the help of a on-board manoeuvre plan or of uplinked commands from the ground station. Phase sequencing may be driven by the state predictor in charge of detecting sensors failures (not treated here). Phase and FDIR signals are not shown in Figure 5.
2) The state predictor is a complex function in charge of predicting the attitude state $\mathbf{x}(t)$ to be compared with the reference data. The state must be at least one-step predicted to allow the control law to compute in advance the attitude command. In practice during the i-th step $t_i \le t < t_{i+1}$ the state $\hat{\mathbf{x}}(t+1)$ is computed. The state variables are defined by the

attitude kinematics and dynamics and by the disturbance models included in the state predictor (Embedded Model). The state includes the attitude, e.g. in the form of a quaternion $\hat{\boldsymbol{q}}$, the angular rate $\hat{\boldsymbol{\omega}}$ in body coordinates and in modern control the vector $\hat{\mathbf{M}}_d$ of the disturbance toques to be cancelled by the control. The state predictor may be driven by the same command $\mathbf{u}(t)$ dispatched to the spacecraft: in this way prediction can continue also in the case of sensor unavailability or failure. When sensors are available state variables are updated from the measurements, in such a way to reduce the model error, i.e. the discrepancy between measurements and model output. When the angular rate is directly measured through gyroscopes as $\mathbf{y}_g$, the state predictor is sometimes simplified to the attitude kinematics driven by the gyro measurements. Attitude measurements $\mathbf{y}_q$ are used to recover the gyro drift. The correction can be implemented in continuous way or in an asynchronous way to reset the drift errors. In absence of gyro measurements, the case treated here, the angular rate is predicted from the attitude. Attitude measurements when obtained by different sensors, sun sensors, horizon sensor, start tracker, .magnetometers, must be combined through an attitude determination algorithm to provide the attitude quaternion $\boldsymbol{y}_q$.

3) The control law determines the control action (torques) necessary to force the tracking error, reference minus prediction, within the specified tolerance (closed-loop command), in addition the predicted disturbance torques can be directly cancelled by including the opposite value $-\hat{\mathbf{M}}_q$. When the reference acceleration is available, especially during a manoeuvre, it is part of the control action. The command torque is converted to actual commands of the actuators (usually voltages or reference values) and dispatched to the actuators. The actuator command vector $\mathbf{u}$ is limited (saturated) within the actuator limits. Because of such limits the computed command may be recomputed to avoid saturation. Actuator limits may include range and skew rate (command increment).

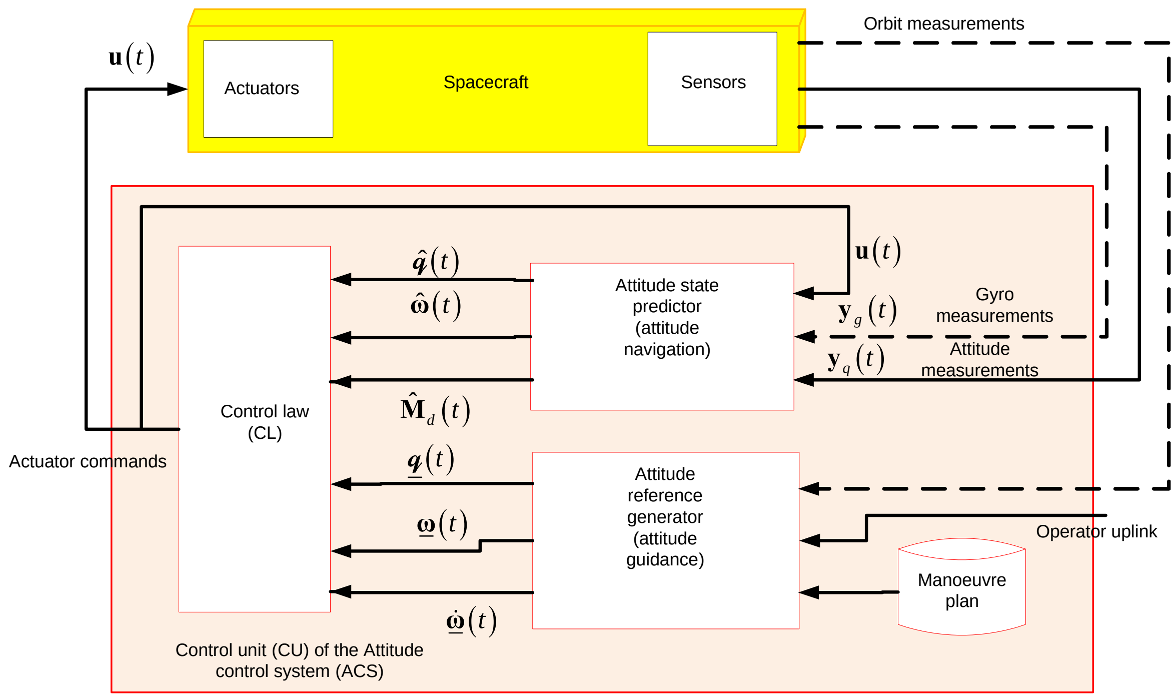

Figure 5. Higher level of the architecture of the control unit of an ACS.

1.5.1 Reference generator

The reference state trajectory must be compatible with the available sensors and actuators. Specifically

1) during orientation manoeuvres (slew manoeuvres) reference accelerations must be such to avoid actuator saturation,
2) the sensor assembly must permit kinematic conditions of the reference trajectory: for instance, if star trackers should be employed, the slew arte must allow the star tracker to supply a continuous attitude determination.

Input signals and data to the reference generator can be rather different

1) A new attitude must be achieved (reorientation): in this case the state and angular acceleration profiles must be generated,
2) The reference attitude is imposed by the orbit itself: for instance the body frame must track the local orbital (LORF) or the local vertical local horizontal frames (LVLH). In this case the reference attitude $\underline{\boldsymbol{q}}$ is given by the quaternion $\boldsymbol{q}_o$ or attitude matrix R_o^i of the orbit frame itself. They must be continuously obtained from the measurement $\mathbf{y}_r$ and $\mathbf{y}_v$ of the spacecraft CoM position $\vec{r}$ and velocity $\vec{v}$ in the inertial frame.

The output signals are

1) reference attitude $\underline{\mathfrak{q}}$, corresponding to the attitude matrix $\underline{R}_b^i$ of the body frame in the inertial frame,
2) reference angular rate $\underline{\boldsymbol{\omega}}$ in the body coordinates,
3) reference angular acceleration $\underline{\mathbf{a}}_q = \underline{\dot{\boldsymbol{\omega}}}$ in the body coordinates.

Reference generators are sometimes called ‘guidance’.

As a case study, the generation of a LORF frame from CoM position and velocity measurements expressed in the inertial frame like the usual J2000 Earth-centered. The LORF is indicated as

$$\mathscr{R}_o = \left\{C, \vec{o}_1, \vec{o}_2, \vec{o}_3\right\}, \tag{5.69}$$

where the origin is the spacecraft CoM, and the axes are defined as in Chapter 3 by

$$\vec{o}_1 = \frac{\vec{v}}{|\vec{v}|},\ \vec{o}_2 = \frac{\vec{h} = \vec{r} \times \vec{v}}{|\vec{h}|},\ \vec{o}_3 = \frac{\vec{e} = \vec{o}_1 \times \vec{o}_2}{|\vec{e}|}. \tag{5.70}$$

The CoM position and velocity are $\vec{r}$ and $\vec{v}$, whereas $\vec{h}$ is orbit angular momentum per mass unit. The three axes are denoted also as roll, pitch and yaw axes.

Denote the CoM measurements as

$$\begin{aligned} \mathbf{y}_r(t) &= \mathbf{r}(t) + \delta\mathbf{r}(t) \\ \mathbf{y}_v(t) &= \mathbf{v}(t) + \delta\mathbf{v}(t) \end{aligned}, \tag{5.71}$$

where inertial position and velocity $\mathbf{r}(t), \mathbf{v}(t)$ are affected by measurement errors.

It is immediate to obtain the LORF attitude matrix from (5.71)

$$\begin{aligned} &\underline{R}_o^i(t) = \begin{bmatrix} \dfrac{\mathbf{y}_v}{y_v} & \dfrac{\mathbf{y}_h = \mathbf{y}_r \times \mathbf{y}_v}{y_h} & \dfrac{\mathbf{y}_e = \mathbf{y}_v \times (\mathbf{y}_r \times \mathbf{y}_v)}{y_e} \end{bmatrix}(t) \\ &y_v = |\mathbf{y}_v|,\ y_h = |\mathbf{y}_r \times \mathbf{y}_v|,\ y_e = |\mathbf{y}_v \times (\mathbf{y}_r \times \mathbf{y}_v)| \end{aligned}. \tag{5.72}$$

The LORF matrix in (5.72) is affected by the GPS errors in (5.71). The error is defined as in chapter 1 through an infinitesimal rotation

$$\begin{aligned} R_o^i &= \underline{R}_o^i\left(I + \delta R_o^i\right) \\ \delta R_o^i &= \begin{bmatrix} 0 & -\delta\theta_{o3} & \delta\theta_{o2} \\ \delta\theta_{o3} & 0 & -\delta\theta_{o1} \\ -\delta\theta_{o2} & \delta\theta_{o1} & 0 \end{bmatrix} = \delta\boldsymbol{\theta}_o \times \end{aligned}. \tag{5.73}$$

An approximate relation between GPS error and LORF is the following

$$\delta\boldsymbol{\theta}_o = \frac{1}{r}\begin{bmatrix} -\delta\vec{r}\cdot\vec{o}_2 \\ \delta\vec{r}\cdot\vec{o}_1 - \delta\vec{v}\cdot\vec{o}_3/\omega_o \\ \delta\vec{v}\cdot\vec{o}_2/\omega_o \end{bmatrix}, v \cong \omega_o r\,. \tag{5.74}$$

Assume GPS error to be white noise and all components to have the same variance,

$$\begin{aligned}\mathcal{E}\left[\delta\mathbf{r}\delta\mathbf{r}^T\right] &= I\sigma_r^2 \\ \mathcal{E}\left[\delta\mathbf{v}\delta\mathbf{v}^T\right] &= I\sigma_v^2\end{aligned}\,. \tag{5.75}$$

Then the covariance of the infinitesimal rotation is approximated by

$$\mathcal{E}\left\{\delta\boldsymbol{\theta}_o\delta\boldsymbol{\theta}_o^T\right\} \cong \begin{bmatrix} (\sigma_r/r)^2 & 0 & 0 \\ 0 & (\sigma_r/r)^2 + (\sigma_v/r\omega_o)^2 & 0 \\ 0 & 0 & (\sigma_v/r\omega_o)^2 \end{bmatrix}, \tag{5.76}$$

where the cross-covariance can be approximated to zero since the rotation errors refer to orthogonal axes. It is now possible to establish the requirements if GPS errors, given the requirements of the reference error. Assume uniform variance for the rotation errors

$$\mathcal{E}\left\{\delta\boldsymbol{\theta}_o\delta\boldsymbol{\theta}_o^T\right\} \le I\sigma_{o,\max}^2\,. \tag{5.77}$$

The most critical component in (5.76) is the second one (pitch, about the orbit normal). Allocating the same variance to both components, one obtains

$$\begin{aligned}\sigma_r &< r\sigma_{o,\max}/\sqrt{2} \cong (R_E + h)\sigma_{o,\max}/\sqrt{2} \\ \sigma_v &< \omega_o r\sigma_{o,\max}/\sqrt{2}\end{aligned}\,. \tag{5.78}$$

Fixing $R_E = 6.38\times10^3$ km, $h = 300$ km and $\omega_o \cong 1.2$ mrad/s, $\sigma_{o,\max} = 0.001$ mrad, one has

$$\begin{aligned}\sigma_r &\le 4.75 \text{ m} \\ \sigma_v &< 0.0057 \text{ m/s}\end{aligned}, \tag{5.79}$$

compatible with GPS errors.

Using the conversion from the attitude matrix to quaternion the reference quaternion $\underline{\mathfrak{q}}_q$ is computed

$$\underline{\mathfrak{q}}_o(t) = \underline{\mathfrak{q}}_o\left(\underline{R}_o^i(t)\right). \tag{5.80}$$

The second step is to compute the reference angular rate. A pair of approaches can be adopted.

1) The attitude matrix derivative defined in Chapter 1 is employed, together with the equation

$$\begin{aligned}&\dot{\underline{R}}_o^i(t) = \underline{R}_o^i(t)\underline{\mathit{\Omega}}_\times(t)\\ &\underline{\mathit{\Omega}}_\times(t) = \underline{\boldsymbol{\omega}}(t)\times\end{aligned}. \tag{5.81}$$

The attitude matrix derivative may be computed as

$$\dot{\underline{R}}_b^i(t) \cong \left(\underline{R}_b^i(t) - \underline{R}_b^i(t-T)\right)/T\ . \tag{5.82}$$

2) The derivative computation in (5.82) is affected by the measurement noise. Noise filtering is performed through a dynamic filter in the form of a Kalman filter or more generically in the form a closed-loop state predictor.

1.5.2 Reference generator as a state predictor

1.5.2.1 Embedded model

The advantage of state predictor are the following

1) the measurement errors in (5.71) can be conveniently filtered to provide a reference quaternion $\underline{\boldsymbol{q}}$ different from (5.80), but possessing the requested accuracy and thus closer the true one,
2) the reference quaternion $\underline{\boldsymbol{q}}$ is predicted together with the orbit angular rate and acceleration vectors; the angular rate vector $\underline{\boldsymbol{\omega}}$ is always nonzero, because of the orbit angular momentum $\vec{h} = \vec{r} \times \vec{v}$ in (5.70). When the orbit is Kepler $\vec{h} = \vec{r} \times \vec{v}$ is constant, but not in presence of perturbations like J2 or drag. In the latter case also the angular acceleration vector $\dot{\underline{\boldsymbol{\omega}}}$ is different from zero and should be retrieved.

Let us start from the quaternion discrete-time state equation in Chapter 1, here reported

$$\boldsymbol{q}(i+1) = \cos\left(\omega(i)T/2\right)\boldsymbol{q}(i) + \frac{1}{2}\frac{\sin\left(\omega(i)T/2\right)}{\omega(t)T/2}\boldsymbol{q}(i)\otimes\boldsymbol{\omega}(i)T\ . \tag{5.83}$$

Equation (5.83) is rewritten in terms of $\underline{\boldsymbol{q}}$ and the angular increment $\underline{\boldsymbol{\omega}}^* = \underline{\boldsymbol{\omega}}T$, through some notation simplifications

$$\begin{aligned}&\underline{\boldsymbol{q}}(i+1) = c(i)\underline{\boldsymbol{q}}(i) + \frac{1}{2}s(i)\underline{\boldsymbol{q}}(i)\otimes\underline{\boldsymbol{\omega}}^*(i),\ \underline{\boldsymbol{q}}(0) = \underline{\boldsymbol{q}}_0\\ &c(i) = \cos\left(\omega^*(i)/2\right),\ \omega^*(i) = \left|\underline{\boldsymbol{\omega}}^*(i)\right|\\ &c(i) = 2\sin\left(\omega^*(i)/2\right)/\omega^*\end{aligned}\ . \tag{5.84}$$

When $\omega^*(i) << 1$, (5.84) equation simplifies because $c(i) \cong s(i) \cong 1$. The angular increment can be interpreted as the average rate during the time unit T

$$\underline{\boldsymbol{\omega}}(i)T = \int_{iT}^{(i+1)T} \boldsymbol{\omega}(\tau)d\tau,\ \underline{\omega}(i) = \left|\underline{\boldsymbol{\omega}}(i)\right|. \tag{5.85}$$

3) Angular rate and accelerations to be predicted must become state variables. This is obtained through a stochastic dynamics driven by white noise as in a generic unknown disturbance model. The noise estimator of the state predictor is in charge of real-time estimating the driving noise. In summary the quaternion kinematic equation (5.83) is complemented by the following disturbance dynamics

$$\begin{bmatrix} \underline{\boldsymbol{\omega}}^* \\ \underline{\mathbf{a}}_q \\ \underline{\mathbf{s}}_q \end{bmatrix}(i+1) = \begin{bmatrix} I & I & 0 \\ 0 & I & 0 \\ 0 & 0 & I \end{bmatrix}\begin{bmatrix} \underline{\boldsymbol{\omega}}^* \\ \underline{\mathbf{a}}_q \\ \underline{\mathbf{s}}_q \end{bmatrix}(i) + \begin{bmatrix} \underline{\mathbf{w}}_\omega \\ \underline{\mathbf{w}}_a \\ \underline{\mathbf{w}}_s \end{bmatrix}(i),\ \begin{bmatrix} \underline{\boldsymbol{\omega}}^* \\ \underline{\mathbf{a}}_q \\ \underline{\mathbf{s}}_q \end{bmatrix}(0) = \begin{bmatrix} \underline{\boldsymbol{\omega}}_0^* \\ 0 \\ 0 \end{bmatrix}, \tag{5.86}$$

where $\underline{\boldsymbol{\omega}}_0^*$ is the nominal orbital angular rate.

Each component $\underline{\omega}_k^*,\ k = 1,2,3$ in (5.86) is decoupled from the other components, if also the components of the white noise vectors are assumed uncorrelated. The state of the stochastic dynamics provide the series of unknown causes generating the orbit quaternion, without any a priori knowledge of them. Equations (5.84) and (5.86) constitute the Embedded Model. All the state variables are quaternion components or angular increments and therefore are either dimensionless or measured in radians.

The noise is estimated from the 'known' model error $\delta\underline{\boldsymbol{q}}$, (measurement less model output) and defined through quaternion multiplication as in Chapter 1

$$\underline{\boldsymbol{y}}_o = \underline{\boldsymbol{q}} \otimes \delta\underline{\boldsymbol{q}} \Rightarrow \delta\underline{\boldsymbol{q}} = \underline{\boldsymbol{q}}^{-1} \otimes \underline{\boldsymbol{y}}_o. \tag{5.87}$$

If one assumes that the model error is kept small by the state predictor, then the latter can be approximated to

$$\delta\underline{\boldsymbol{q}} = \begin{bmatrix} \delta\underline{q}_0 \\ \delta\underline{\mathbf{q}} \end{bmatrix} \cong \begin{bmatrix} 1 \\ \delta\underline{\theta}_1/2 \\ \delta\underline{\theta}_2/2 \\ \delta\underline{\theta}_3/2 \end{bmatrix} = \begin{bmatrix} 1 \\ \delta\underline{\boldsymbol{\theta}}/2 \end{bmatrix}, \tag{5.88}$$

where $\delta q_0 \cong 1 >> \left|\delta\underline{\mathbf{q}}\right|$.

1.5.2.2 Reference generator error equation

Equation (5.84) is nonlinear, but it was shown in Chapter 1 that a quaternion error can be expressed as the state variable of an error equation very close to be linear around zero error defined by $\delta\underline{q}_0 = 1,\ \delta\underline{\mathbf{q}} = 0$. To this end we distinguish between the model output $\underline{\boldsymbol{q}}$, known and to be used by the control itself as a reference quaternion, and the 'true' quaternion $\boldsymbol{q}_{true}$, unknown. The reference generator error (reference quaternion – 'true' quaternion) is defined in a similar way as (5.87)

$$\underline{\boldsymbol{q}} = \boldsymbol{q}_{true} \otimes \delta \boldsymbol{q}_{true} \Rightarrow \delta \boldsymbol{q}_{true} = \boldsymbol{q}_{true}^{-1} \otimes \underline{\boldsymbol{q}} . \tag{5.89}$$

In a similar way, we represent the quaternion error through Euler angles as

$$\delta \boldsymbol{q}_{true} = \begin{bmatrix} \delta q_{true,0} \\ \delta \mathbf{q}_{true} \end{bmatrix} \cong \begin{bmatrix} 1 \\ \delta \boldsymbol{\theta}_{true} / 2 \end{bmatrix}. \tag{5.90}$$

Following the error equation in Chapter 1, eq. (1.198), which is reported in terms of $\delta \mathbf{q}_{true}$ after conversion to DT

$$\begin{aligned} &\frac{\delta \mathbf{q}_{true}(i+1) - \delta \mathbf{q}_{true}(i)}{T} \cong -\underline{\boldsymbol{\omega}}(i) \times \delta \mathbf{q}_{true}(i) + \frac{1}{2} \delta \underline{\boldsymbol{\omega}}_{true}(i),\ \delta \mathbf{q}_{true}(0) = \delta \mathbf{q}_{true,0}, \\ &\delta \underline{\boldsymbol{\omega}}_{true} = \underline{\boldsymbol{\omega}} - \boldsymbol{\omega}_{true} \end{aligned} \tag{5.91}$$

we can write the linear DT equation

$$\delta \boldsymbol{\theta}_{true}(i+1) = \left(I - \underline{\boldsymbol{\omega}} T \times\right) \delta \boldsymbol{\theta}_{true}(i) + \delta \underline{\boldsymbol{\omega}}_{true}^{*}(i),\ \delta \boldsymbol{\theta}_{true}(0) = \delta \boldsymbol{\theta}_{true,0}, \tag{5.92}$$

where the error increment $\delta \underline{\boldsymbol{\omega}}_{true}^{*}$ is the error between the model and the 'true' orbital rate $\boldsymbol{\omega}_{true}$. Assuming $\left|\boldsymbol{\omega} T\right| << 1$ equation (5.92) is approximated to

$$\delta \boldsymbol{\theta}_{true}(i+1) = \delta \boldsymbol{\theta}_{true}(i) + \delta \underline{\boldsymbol{\omega}}_{true}^{*}(i),\ \delta \boldsymbol{\theta}_{true}(0) = \delta \boldsymbol{\theta}_{true,0}, \tag{5.93}$$

but the approximation must be accounted for when designing the noise estimator. The unknown rate error $\delta \underline{\boldsymbol{\omega}}_{true}^{*}$ can be described by a stochastic dynamics as in (5.86). Since the state coordinates in (5.93) and in (5.86) are decoupled, the ensemble of both equations split into three separate fourth order equations

$$\begin{bmatrix} \delta \theta_{true} \\ \delta \underline{\omega}_{true}^{*} \\ \underline{a}_q \\ \underline{s}_q \end{bmatrix}(i+1) = \begin{bmatrix} 1 & 1 & 0 & 0 \\ 0 & 1 & 1 & 0 \\ 0 & 0 & 1 & 1 \\ 0 & 0 & 0 & 1 \end{bmatrix} \begin{bmatrix} \delta \theta_{true} \\ \delta \underline{\omega}_{true}^{*} \\ \underline{a}_q \\ \underline{s}_q \end{bmatrix}(i) + \begin{bmatrix} 0 \\ \underline{w}_{\omega} \\ \underline{w}_a \\ \underline{w}_s \end{bmatrix}(i),\ \begin{bmatrix} \delta \theta_{true} \\ \delta \underline{\omega}_{true}^{*} \\ \underline{a}_q \\ \underline{s}_q \end{bmatrix}(0) = \begin{bmatrix} \delta \theta_{true,0} \\ 0 \\ 0 \\ 0 \end{bmatrix}, \tag{5.94}$$

where the subscript $k = 1,2,3$ has been dropped, and the (differential) measurement and model error have to be defined.

Remarks. Equation (5.94) can be viewed as the linearization of (5.83) and (5.86) in the neighbourhood of the 'true' orbit. Perturbations are expressed as the output of 3rd order stochastic process driven by white noise to be retrieved from measurements. A circular orbit can be viewed also as the response of the quaternion kinematics driven by a constant angular rate.

The measurement error ('true' model error) $\delta\boldsymbol{y}$ is a component of the quaternion error between the measurement and the 'true' quaternion

$$\boldsymbol{y}_o = \boldsymbol{q}_{true} \otimes \delta\boldsymbol{y} \Rightarrow \delta\boldsymbol{y} = \boldsymbol{q}_{true}^{-1} \otimes \boldsymbol{y}_o . \quad (5.95).$$

Combining (5.95) and (5.89), the 'known' model error in (5.87) is obtained

$$\begin{aligned} \delta\underline{\boldsymbol{q}} &= \underline{\boldsymbol{q}}^{-1} \otimes \underline{\boldsymbol{y}}_o = \delta\boldsymbol{q}_{true}^{-1} \otimes \boldsymbol{q}_{true}^{-1} \otimes \underline{\boldsymbol{y}}_o = \delta\boldsymbol{q}_{true}^{-1} \otimes \delta\boldsymbol{y} \\ \delta\boldsymbol{y} &\cong \begin{bmatrix} 1 \\ \delta\mathbf{y} = \delta\boldsymbol{\theta}_y / 2 \end{bmatrix} \end{aligned} . \quad (5.96).$$

But quaternion multiplication between two error quaternions leads, neglecting second order terms, to

$$\delta\boldsymbol{q}_{true}^{-1} \otimes \delta\boldsymbol{y} = \begin{bmatrix} \delta q_{true,0}\delta y_0 + \delta\mathbf{q}_{nom}^T \delta\mathbf{y} \\ \hline \delta q_{true,0}\delta\mathbf{y} - \delta y_0 \delta\mathbf{q}_{true} - \delta\mathbf{q}_{true} \times \delta\mathbf{y} \end{bmatrix} \cong \begin{bmatrix} 1 \\ \hline \delta\mathbf{y} - \delta\mathbf{q}_{true} \end{bmatrix} \cong \begin{bmatrix} 1 \\ \hline \delta\underline{\mathbf{q}} \end{bmatrix}, \quad (5.97)$$

and to a scalar equation

$$\delta\underline{\theta} = \delta\theta_y - \delta\theta_{true} . \quad (5.98)$$

The last equation can be read as measurement-reference quaternion (known model error) equals (measurement – 'true' quaternion) (model error) minus (reference -'true' quaternion). Equation (5.98) can be rewritten in terms of the state variables in (5.94) as

$$\delta\theta_y(i) = \begin{bmatrix} 1 & 0 & 0 & 0 \end{bmatrix} \begin{bmatrix} \delta\theta_{true} \\ \delta\underline{\omega}_{true}^* \\ \underline{a}_q \\ \underline{s}_q \end{bmatrix} (i) + \delta\underline{\theta}(i), \quad (5.99)$$

where the model error is the sum of the reference generator error and the measurement error. The measurement error $\delta\underline{\theta}$ becomes the source of the noise estimator applied to equation (5.94).

Remarks. Important. Notice that the model error in (5.94) is the same in (5.87) less the scale factor 0.5, which suggests that the implementation, although designed through (5.94) in the linear framework, can be made on the original (nonlinear) equations, since the noise vectors remain the same as the model error!

1.5.2.3 The noise estimator

One can now proceed to design the noise estimator for the Embedded model (5.94).

The immediate problem to be solved is the reduced size of the noise vector, $n_w = 3$, wrt to the state size $n = 4$, in the case the noise vector in (5.94) should be respected. We shall follow this way and we shall show how to overcome the difficulty. An alternative way typical of Kalman filter is to add a noise also on the first row in (5.94).

Start by a static noise estimator of size n_w, which amounts to

$$\begin{bmatrix} \underline{w}_\omega \\ \underline{w}_a \\ \underline{w}_s \end{bmatrix}(i) = \begin{bmatrix} \underline{l}_\omega \\ \underline{l}_a \\ \underline{l}_s \end{bmatrix}\delta\underline{\theta}(i) = \begin{bmatrix} \underline{l}_\omega \\ \underline{l}_a \\ \underline{l}_s \end{bmatrix}\left(\delta\theta_y(i) - \delta\theta_{true}(i)\right). \tag{5.100}$$

The closed loop equation, combination of (5.94) and (5.100), results

$$\begin{bmatrix} \delta\theta_{true} \\ \delta\underline{\omega}^*_{true} \\ \underline{a}_q \\ \underline{s}_q \end{bmatrix}(i+1) = \begin{bmatrix} 1 & 1 & 0 & 0 \\ -\underline{l}_\omega & 1 & 1 & 0 \\ -\underline{l}_a & 0 & 1 & 1 \\ -\underline{l}_s & 0 & 0 & 1 \end{bmatrix}\begin{bmatrix} \delta\theta_{true} \\ \delta\underline{\omega}^*_{true} \\ \underline{a}_q \\ \underline{s}_q \end{bmatrix}(i) + \begin{bmatrix} 0 \\ \underline{l}_\omega \\ \underline{l}_a \\ \underline{l}_s \end{bmatrix}\delta\theta_y(i),\ \begin{bmatrix} \delta\theta_{true} \\ \delta\underline{\omega}^*_{true} \\ \underline{a}_q \\ \underline{s}_q \end{bmatrix}(0) = \begin{bmatrix} \delta\theta_{true,0} \\ 0 \\ 0 \\ 0 \end{bmatrix}. \tag{5.101}$$

The following theorem can be proved by computing the characteristic polynomial.

Theorem 1. There is no feedback gain capable of stabilizing (5.101).

Proof. Compute the characteristic polynomial of the state matrix in (5.101) using $\gamma = \lambda - 1$, resulting into

$$\begin{aligned} &\det\begin{bmatrix} \gamma & -1 & 0 & 0 \\ \underline{l}_\omega & \gamma & -1 & 0 \\ \underline{l}_a & 0 & \gamma & -1 \\ \underline{l}_s & 0 & 0 & \gamma \end{bmatrix} = \gamma^4 + \det\begin{bmatrix} \underline{l}_\omega & -1 & 0 \\ \underline{l}_a & \gamma & -1 \\ \underline{l}_s & 0 & \gamma \end{bmatrix} =, \\ &= \gamma^4 + \underline{l}_\omega\gamma^2 + \underline{l}_a\gamma + \underline{l}_s \end{aligned} \tag{5.102}$$

and equal the coefficients $c_k,\ k = 3,2,1,0$ to those obtained by fixing four complementary eigenvalues

$$\Gamma = \{\gamma_1, \ldots, \gamma_4\} \tag{5.103}$$

Clearly the third-order coefficients in (5.102) is zero and equal the sum of the eigenvalues as follows

$$0 = c_3 = \gamma_1 + \gamma_2 + \gamma_3 + \gamma_4, \tag{5.104}$$

which implies at least a negative eigenvalue, say $\gamma_k < 0$. But

$$\gamma_k = 1 - \lambda_k \Rightarrow \lambda_k = 1 - \gamma_k \Rightarrow |\lambda_k| > 1 \tag{5.105}$$

showing at least one eigenvalue becomes unstable.

The theorem can be bypassed by adding a second model error, denoted as $\delta \underline{p}$, which is correlated but linearly independent of $\delta\underline{\theta}$, and by completing the noise estimator with a static function of $\delta \underline{p}$, as follows

$$\begin{bmatrix} \underline{w}_\omega \\ \underline{w}_a \\ \underline{w}_s \end{bmatrix}(i) = \begin{bmatrix} \underline{l}_\omega \\ \underline{l}_a \\ \underline{l}_s \end{bmatrix}\delta\underline{\theta}(i) + \begin{bmatrix} \underline{m}_\omega \\ \underline{m}_a \\ \underline{m}_s \end{bmatrix}\delta\underline{p}(i). \tag{5.106}$$

The second error independence is obtained through a 1st order dynamics

$$\delta\underline{p}(i+1) = (1-\underline{\beta})\delta\underline{p}(i) + \delta\underline{\theta}(i),\ \delta\underline{p}(0) = 0 \tag{5.107}$$

which makes the noise estimator a dynamic feedback. It can be shown now that if the complementary eigenvalue $\underline{\beta}$ is free, the state predictor can be stabilized. The latter becomes of the 5th order as follows

$$\begin{bmatrix} \delta\theta_{true} \\ \delta\underline{\omega}^*_{true} \\ \underline{a}_q \\ \underline{s}_q \\ \delta\underline{p} \end{bmatrix}(i+1) = \begin{bmatrix} 1 & 1 & 0 & 0 & 0 \\ -\underline{l}_\omega & 1 & 1 & 0 & \underline{m}_\omega \\ -\underline{l}_a & 0 & 1 & 1 & \underline{m}_a \\ -\underline{l}_s & 0 & 0 & 1 & \underline{m}_s \\ -1 & 0 & 0 & 0 & 1-\underline{\beta} \end{bmatrix}\begin{bmatrix} \delta\theta_{true} \\ \delta\underline{\omega}^*_{true} \\ \underline{a}_q \\ \underline{s}_q \\ \delta\underline{p} \end{bmatrix}(i) + \begin{bmatrix} 0 \\ \underline{l}_\omega \\ \underline{l}_a \\ \underline{l}_s \\ 1 \end{bmatrix}\delta\theta_y(i),\ \begin{bmatrix} \delta\theta_{true} \\ \delta\underline{\omega}^*_{true} \\ \underline{a}_q \\ \underline{s}_q \\ \delta\underline{p} \end{bmatrix}(0) = \begin{bmatrix} \delta\theta_{true,0} \\ 0 \\ 0 \\ 0 \\ 0 \end{bmatrix}. \tag{5.108}$$

Theorem 2. By leaving $\underline{\beta}$ free, the eigenvalues of (5.108) can be arbitrarily assigned.

Proof. Compute the characteristic polynomial

$$\begin{aligned} &\det\begin{bmatrix} \gamma & -1 & 0 & 0 & 0 \\ \underline{l}_\omega & \gamma & -1 & 0 & -\underline{m}_\omega \\ \underline{l}_a & 0 & \gamma & -1 & -\underline{m}_a \\ \underline{l}_s & 0 & 0 & \gamma & -\underline{m}_s \\ 1 & 0 & 0 & 0 & \gamma+\underline{\beta} \end{bmatrix} = \gamma^4(\gamma+\underline{\beta}) + \det\begin{bmatrix} \underline{l}_\omega & -1 & 0 & -\underline{m}_\omega \\ \underline{l}_a & \gamma & -1 & -\underline{m}_a \\ \underline{l}_s & 0 & \gamma & -\underline{m}_s \\ 1 & 0 & 0 & \gamma+\underline{\beta} \end{bmatrix} = \\ &= \gamma^4(\gamma+\underline{\beta}) + (\underline{l}_\omega\gamma^2 + \underline{l}_a\gamma + \underline{l}_s)(\gamma+\underline{\beta}) + \underline{m}_\omega\gamma^2 + \underline{m}_a\gamma + \underline{m}_s = \\ &= \gamma^5 + \gamma^4\underline{\beta} + \gamma^3\underline{l}_\omega + \gamma^2(\underline{m}_\omega + \underline{l}_\omega\underline{\beta} + \underline{l}_a) + \gamma(\underline{m}_a + \underline{l}_a\underline{\beta} + \underline{l}_s) + \underline{m}_s + \underline{l}_s\underline{\beta} \end{aligned}. \tag{5.109}$$

It shows that having fixed five complementary eigenvalues

$$\Gamma = \{\gamma_1, \ldots, \gamma_5\} \tag{5.110}$$

the fourth order coefficients in (5.109) is given by

$$c_4 = \gamma_1 + \gamma_2 + \gamma_3 + \gamma_4 = \underline{\beta}, \tag{5.111}$$

and implies $\underline{\beta}$ must be free.

Theorem 3. The characteristic equation in (5.109) includes a pair of free coefficients, since there are seven gains for five coefficients. The simplest choice is within the pairs $\left(\underline{m}_\omega, \underline{l}_a\right)$ and $\left(\underline{m}_a, \underline{l}_s\right)$, and amounts to set either coefficient of each pair to zero.

Proof. The proof is immediate. The usual choice is the following

$$\underline{l}_a = \underline{l}_s = 0\,, \tag{5.112}$$

which corresponds to estimate $\underline{w}_a$ and $\underline{w}_s$ from the second model error δp only.

1.5.2.4 Predictor transfer function

Restricting to a single DoF, the LTI equation (5.108) can be easily converted to a transfer function (TF), by separating three blocks

1) the block from the total acceleration $a_{q,tot}$ to the differential attitude $\delta\theta_{true}$ (model-nominal), free of noise, and consisting of the cascade of two adders, leading to the TF

$$\delta\theta_{nom}\left(z\right) = \left(z-1\right)^{-2} \underline{a}_{tot}\left(z\right) = \underline{\mathbf{M}}\left(z\right) a_{tot}\left(z\right) \tag{5.113}$$

2) the multivariate block from the noise vector $\mathbf{w}$ to the total acceleration

$$\underline{a}_{tot}\left(z\right) = \begin{bmatrix} 1 & \left(z-1\right)^{-1} & \left(z-1\right)^{-2} \end{bmatrix} \begin{bmatrix} \underline{w}_\omega \\ \underline{w}_a \\ \underline{w}_s \end{bmatrix} = \underline{\mathbf{D}}\left(z\right)\underline{\mathbf{w}}\left(z\right) \tag{5.114}$$

3) the dynamic noise estimator

$$\underline{\mathbf{w}}\left(z\right) = \left(\begin{bmatrix} \underline{l}_\omega \\ 0 \\ 0 \end{bmatrix} + \frac{1}{z-1+\underline{\beta}} \begin{bmatrix} \underline{m}_\omega \\ \underline{m}_a \\ \underline{m}_s \end{bmatrix}\right)\left(\delta\theta_y - \delta\theta_{true}\right)\left(z\right) = \underline{\mathbf{L}}\left(z\right)\left(\delta\theta_y - \delta\theta_{true}\right)\left(z\right). \tag{5.115}$$

Denoting with $\mathbf{H} = \mathbf{DL}$ the overall feedback from model error to the total acceleration, one easily obtains the closed loop expression

$$\delta\theta_{nom}\left(z\right) = \left(I + \underline{\mathbf{M}}\underline{\mathbf{H}}\right)^{-1} \underline{\mathbf{M}}\underline{\mathbf{H}}\delta\theta_y\left(z\right) = \underline{\mathbf{V}}\delta\theta_y\left(z\right) = \left(I - \underline{\mathbf{S}}\right)\delta\theta_y\left(z\right), \tag{5.116}$$

where sensitivity and the complement have been defined.

Moreover the differential measurement $\delta\theta_y$ (measurement –nominal) defined in (5.95), is defined in (5.94) as the sum of the model output and the model error $\delta\underline{\theta}$. The model output in (5.94) must not be confused with $\delta\theta_{true}$ in (5.116) and (5.108), since the latter is the 'known' result of the noise estimator, whereas the former is the 'unknown' output of a stochastic model, encompassing all the possible realizations. Using the same notations as above one can write

$$\delta\theta_y(z) = \underline{\mathbf{M}}\underline{\mathbf{D}}\underline{\mathbf{w}}(z) + \delta\underline{\theta}(z), \tag{5.117}$$

where $\underline{\mathbf{w}}$ is the set of all possible noise realization. The former term in (5.117) must be tracked by $\delta\theta_{true}$ as it is the model, whereas the latter term must be rejected being the model error. Since $\underline{\mathbf{V}}$ is a low pass filter, only the higher frequency components of $\delta\underline{\theta}$ can be rejected. Measurement errors due to GPS are part of the model error. Their effect on $\delta\theta_{nom}$ and $\boldsymbol{q}$ can be attenuated by restricting the BW of $\underline{\mathbf{V}}$ and making the higher-frequency decreasing slope as sharp as possible. A dynamic estimator is favouring a sharper slope.

The explicit expressions of the loop transfer function $\underline{\mathbf{M}}\underline{\mathbf{H}}$ and of the complementary sensitivity $\underline{\mathbf{V}}$ are the following

$$\begin{aligned}\underline{\mathbf{M}}(z)\underline{\mathbf{H}}(z) &= \left(\underline{l}_\omega + \left(\underline{m}_\omega + \frac{\underline{m}_a}{z-1} + \frac{\underline{m}_s}{(z-1)^2}\right)\frac{1}{z-1+\underline{\beta}}\right)\frac{1}{(z-1)^2} = \\ &= \frac{(z-1)^2\left(\underline{l}_\omega\left(z-1+\underline{\beta}\right)+\underline{m}_\omega\right)+(z-1)\underline{m}_a+\underline{m}_s}{(z-1)^4\left(z-1+\underline{\beta}\right)}\end{aligned} \tag{5.118}$$

and

$$\underline{\mathbf{V}} = \left(I + \underline{\mathbf{M}}\underline{\mathbf{H}}\right)^{-1}\underline{\mathbf{M}}\underline{\mathbf{H}} = \frac{(z-1)^2\left(\underline{l}_\omega\left(z-1+\underline{\beta}\right)+\underline{m}_\omega\right)+(z-1)\underline{m}_a+\underline{m}_s}{(z-1)^4\left(z-1+\underline{\beta}\right)+(z-1)^2\left(\underline{l}_\omega\left(z-1+\underline{\beta}\right)+\underline{m}_\omega\right)+(z-1)\underline{m}_a+\underline{m}_s} \tag{5.119}$$

The high frequency asymptote $z-1\to\infty$ provides both shape (2nd degree) and the approximate BW as follows

$$\begin{aligned}&\lim_{z-1\to\infty}\underline{\mathbf{V}}(z) = \frac{\underline{l}_\omega}{(z-1)^2} \Rightarrow \\ &\lim_{|f|\to\infty,|f|<f_{\max}}\left|\underline{\mathbf{V}}(jf)\right| = \frac{\underline{l}_\omega}{(2\pi fT)^2} = \left(\frac{\underline{f}}{f}\right)^2\end{aligned} \tag{5.120}$$

where $\underline{f} = (2\pi T)^{-1}\sqrt{\underline{l}_\omega}$ is the approximate BW.

Assuming equal eigenvalues $\underline{\gamma}$ in (5.109) for simplicity's sake, it holds

$$\underline{l}_\omega = c_3 = \gamma_1(\gamma_2+\gamma_3+\gamma_4+\gamma_5)+\gamma_2(\gamma_3+\gamma_4+\gamma_5)+\gamma_3(\gamma_4+\gamma_5)+\gamma_4\gamma_5 = 10\underline{\gamma}^2 \tag{5.121}$$

and

$$\underline{f} = \frac{\sqrt{10}\underline{\gamma}}{2\pi T} \tag{5.122}$$

It is now possible to relate performance to eigenvalue, by assuming the measurement errors (if white noise) are attenuated by the factor

$$\varphi \le \sqrt{\frac{\underline{f}}{f_{\max}}} = \sqrt{\frac{\sqrt{10}\underline{\gamma}}{2\pi T \times 0.5/T}} = \sqrt{\frac{\sqrt{10}\underline{\gamma}}{\pi}} \Rightarrow \underline{\gamma} \ge \frac{\pi\varphi^2}{\sqrt{10}} \cong \varphi^2 . \tag{5.123}$$

Remarks. Equal eigenvalues tend to make $\underline{\mathbf{V}}$ to overshoot above unit. To reduce overshoot defined as $\max_f \left|\underline{\mathbf{V}}(jf)\right| - 1$, eigenvalues must be different and separated as in Table 1 and Figure 6. Notice however the significant overshoot of the sensitivity, that here is of no concern.

Table 1. Reference generator design

No	Parameter	Symbol	Unit	Value	Comments
0	Low frequency eigenvalues	$\underline{\gamma}_1, \underline{\gamma}_2, \underline{\gamma}_3$		0.002	Complementary
1	High frequency	$\underline{\gamma}_4, \underline{\gamma}_5$		0.5	idem
2	BW	$\underline{f}$	Hz	0.08	
3	Time unit	T	s	1	
4	Overshoot			<0.025	$\max_f \left|\underline{\mathbf{V}}(jf)\right| - 1$
5	Attenuation	φ		0.4	eq. (5.123)
6	Single eigenvalue	$\underline{\gamma}_k$		0.16	same attenuation
7	Overshoot			< 0.22	

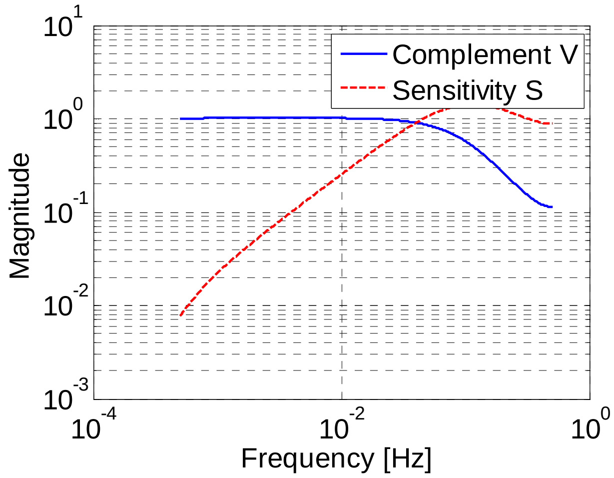

Figure 6. Sensitivity and complement under separated eigenvalues.

Figure 7 compare the complement under separated and single eigenvalue at the same attenuation φ. Separate eigenvalues approach a low pass filter.

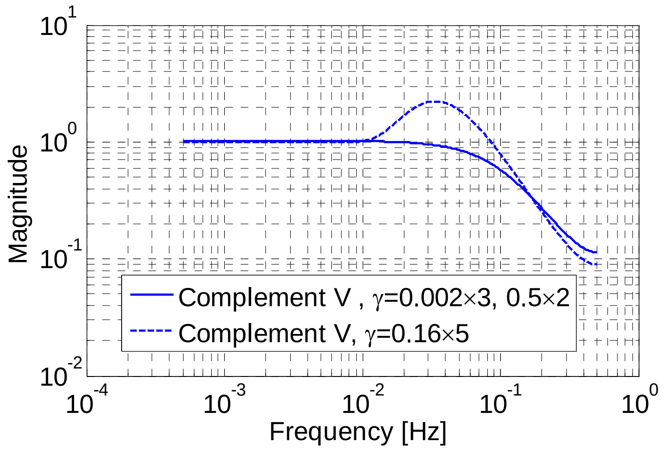

Figure 7. Comparison between separated and single eigenvalue.

1.5.2.5 Mechanization and results

As already said the noise estimator is applied to the quaternion error $\delta\underline{\boldsymbol{q}}$ in (5.87). To this end the vector component $\delta\underline{\boldsymbol{\theta}}$ is extracted from $\delta\underline{\boldsymbol{q}}$ through (5.88), or more accurately through

$$\delta\underline{\boldsymbol{\theta}} = 2\delta\underline{\mathbf{q}} / \delta\underline{q}_0 . \qquad (5.124)$$

The whole block-diagram is in Figure 8.

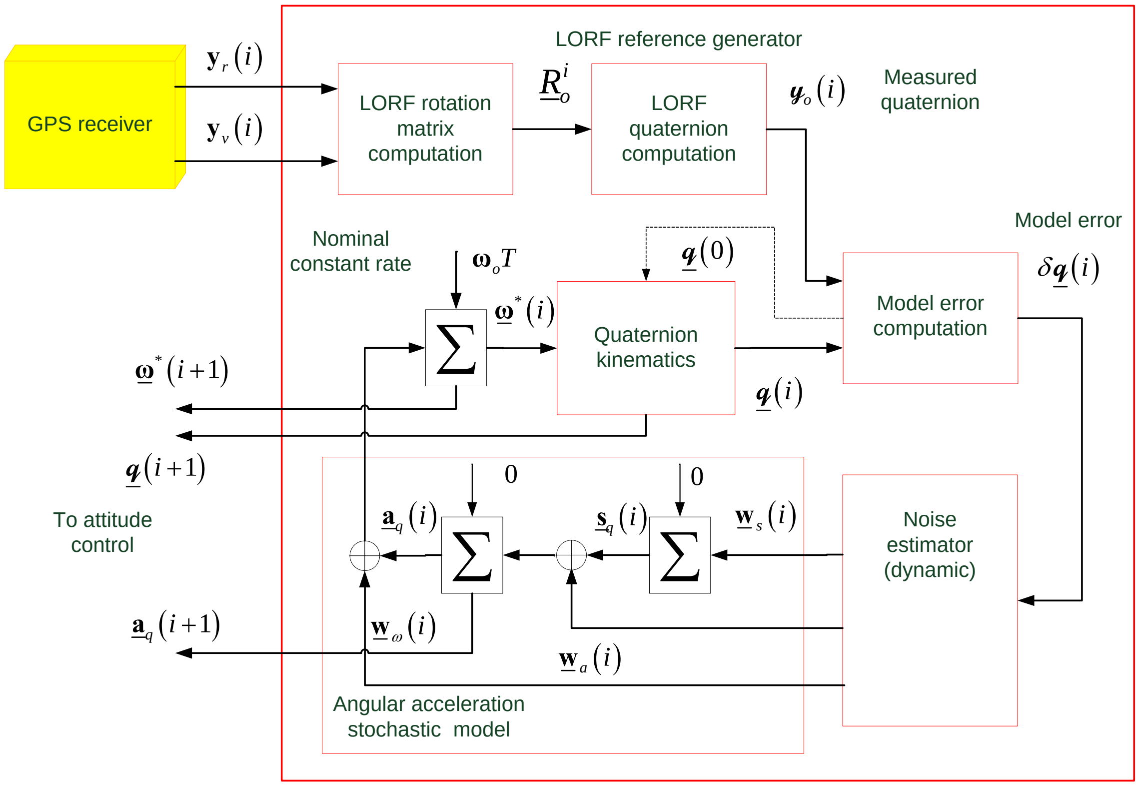

Figure 8. Block-diagram of the LORF reference generator.

Figure 9 shows the angular rate components along a single orbit, under spherical and oblate gravity, i.e. including the J2 component. In both cases the axial (x) component is null, the yaw component (z) is non null in the oblate case, the pitch component around the orbit normal (y) has been cleaned of the mean orbit rate ω_o in the spherical case.

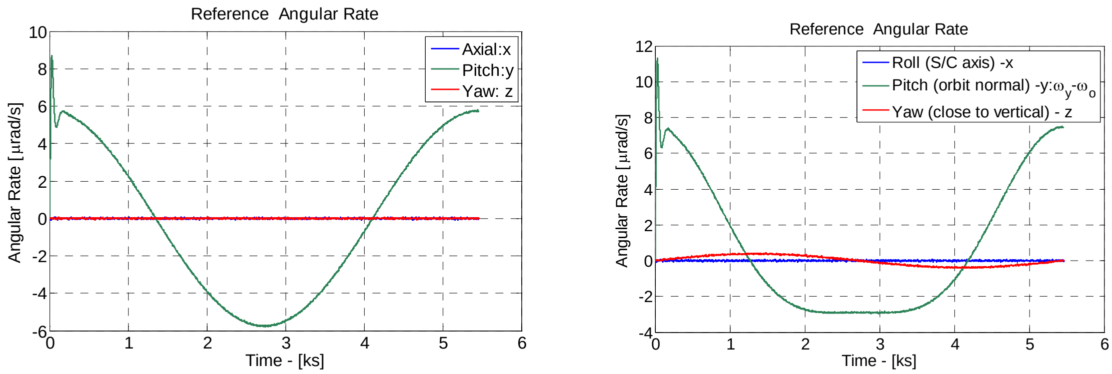

Figure 9. Orbit angular rate (in orbital axes) by the reference generator. Left: spherical gravity. Right: Earth oblateness.

Figure 10 shows the model error of the reference generator for the second component (pitch, about the orbit normal). It is compare with the simulated (‘true’) less reconstructed. The former is mainly due to GPS measurement errors; the latter shows the reconstructed quaternion $\underline{\boldsymbol{q}}$ is very close to the 'true' one and free of measurement errors, as expected by the filter design. The initial transient is due to inaccurate initial value of the pitch angular rate (the orbital rate).

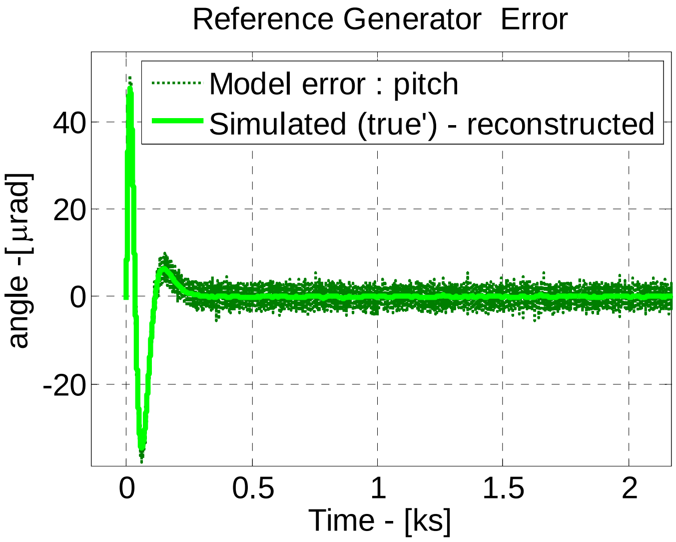

Figure 10. Reference generator: model error and simulated less reconstructed.

1.5.3 State predictor (navigation)

It is sometimes called navigation. Given the reference quaternion (LORF) with angular rate and acceleration, the next issue is to measure spacecraft quaternion, angular rate and unknown disturbance. The same architecture, concept and algorithm adopted for the reference generator is repeated here, with the following exceptions

1) The quaternion measurement $\boldsymbol{y}_q(i)$ is provided by an attitude sensor and specifically by a star tracker, and is corrupted by a measurement error as follows $\boldsymbol{e}_q$

$$\boldsymbol{y}_q(i) = \boldsymbol{q}_b(i) \otimes \boldsymbol{e}_q(i), \tag{5.125}$$

   and $\boldsymbol{q}_b$ is the body frame (principal axes) quaternion in the inertial frame.

2) The total acceleration is the sum of the commanded acceleration $\mathbf{a}_c$ (known, provided by thrusters) and of the disturbance $\mathbf{d}_q$, including gyro, drag, gravity gradient and thruster noise. Part of them may be treated as known components, but some unknown components remain to be described by the same stochastic dynamics as in (5.86). Here all disturbance components are treated as unknown.

3) The noise estimator is designed under LTI assumption as in Section 1.5.2.3, but the nominal quaternion here is not that resulting from the circular orbit, but rather the reference quaternion $\underline{\boldsymbol{q}}$ itself. In this sense the disturbance model accounts for the

environment torques forcing the spacecraft attitude to misalign wrt to the LORF one. The details of the linearization will not be provided as already reported above.

1.5.3.1 Embedded Model

The Embedded Model is the same as (5.83) and (5.86), with the addition of the command $\mathbf{a}_u$. It may be compacted in a single (nonlinear) equation as follows

$$\begin{bmatrix} \boldsymbol{q}_b \\ \boldsymbol{\omega}^* \\ \mathbf{a}_q \\ \mathbf{s}_q \end{bmatrix}(i+1) = \begin{bmatrix} Ic(i) & \dfrac{s(i)}{2}\hat{\boldsymbol{q}}_b(i)\otimes & 0 & 0 \\ 0 & I & I & 0 \\ 0 & 0 & I & I \\ 0 & 0 & 0 & I \end{bmatrix}\begin{bmatrix} \boldsymbol{q}_b \\ \boldsymbol{\omega}^* \\ \mathbf{a}_q \\ \mathbf{s}_q \end{bmatrix}(i) + \begin{bmatrix} 0 \\ I \\ 0 \\ 0 \end{bmatrix}\mathbf{a}_c(i) + \begin{bmatrix} 0 & 0 & 0 \\ I & 0 & 0 \\ 0 & I & 0 \\ 0 & 0 & I \end{bmatrix}\begin{bmatrix} \mathbf{w}_\omega \\ \mathbf{w}_a \\ \mathbf{w}_s \end{bmatrix}(i)$$

$$\begin{bmatrix} \boldsymbol{q}_b \\ \boldsymbol{\omega}^* \\ \mathbf{a}_q \\ \mathbf{s}_q \end{bmatrix}(0) = \begin{bmatrix} \boldsymbol{q}_{b0} \\ \boldsymbol{\omega}^*_0 \\ \mathbf{a}_{q0} \\ \mathbf{s}_{q0} \end{bmatrix} \qquad .(5.126)$$

$$\boldsymbol{y}_q(i) = \boldsymbol{q}_b(i)\otimes\delta\boldsymbol{q}_b(i)$$

The second equation follows from the discretization of the attitude dynamics which is still critical as it is nonlinear because of the gyroscopic torque (and a possible perturbation dependence on the attitude). Discretization can be made by assuming the perturbations are in their great part cancelled by the command torques, that makes the residual nonlinearities weak. Let us partition the external torque in Chapter 2 (2.42) between command and disturbance

$$\mathbf{M}(t) = \mathbf{M}_c(t) + \mathbf{M}_d(t) \qquad (5.127)$$

and express the command as

$$\mathbf{M}_c(t) = -\hat{\mathbf{M}}_d(t) + \hat{\boldsymbol{\omega}}(t)\times \underline{J}\hat{\boldsymbol{\omega}}(t) + \mathit{\Delta}\mathbf{M}_c(t), \qquad (5.128)$$

where $\mathit{\Delta}\mathbf{M}_c$ is the command term to be designed, and $-\hat{\mathbf{M}}_d(t) + \hat{\boldsymbol{\omega}}(t)\times \underline{J}\hat{\boldsymbol{\omega}}(t)$ is the known disturbance part as provided by the state predictor. The dynamics can be rewritten as

$$\dot{\boldsymbol{\omega}}(t) = J^{-1}\left(\mathit{\Delta}\mathbf{M}_c(t) + \mathit{\Delta}\mathbf{M}_d(t)\right),\ \boldsymbol{\omega}(0) = \boldsymbol{\omega}_0, \qquad (5.129)$$

and now can be integrated to provide

$$\begin{aligned}&\boldsymbol{\omega}^*(i+1)=\boldsymbol{\omega}^*(i)+\mathbf{a}_u(i)+B_q\Delta\mathbf{M}_c(i)+\mathbf{a}_q(i)+\mathbf{w}_\omega(i)\\&\mathbf{a}_u(i)=\underline{J}^{-1}T^2\Delta\mathbf{M}_c(i)\\&\mathbf{a}_q(i)+\mathbf{w}_\omega(i)=J^{-1}T\int_{iT}^{(i+1)T}\Delta\mathbf{M}_d(\tau)d\tau\end{aligned}. \tag{5.130}$$

In (5.130), $\underline{J}$ denotes the known inertia matrix, and the residual (unknown) disturbance $\Delta\mathbf{M}_d$ has been integrated to provide a pair of stochastic components, the predictable $\mathbf{a}_q$ and the unpredictable $\mathbf{w}_\omega$. The predictable component is in turn driven by other predictable and unpredictable components. Notice that the quaternion equation in (5.126) requires the average rate (5.85) instead of $\boldsymbol{\omega}^*(i)$, which is the state variable in (5.130). Using the mean value theorem (5.85) can be approximated as

$$\underline{\boldsymbol{\omega}}(i)\cong\boldsymbol{\omega}(i)+\dot{\boldsymbol{\omega}}(i)h,\ 0\le h<T\,. \tag{5.131}$$

The latter can be further approximated assuming $h=0$ as

$$\underline{\boldsymbol{\omega}}(i)\cong\boldsymbol{\omega}(i) \tag{5.132}$$

or by making explicit $\dot{\boldsymbol{\omega}}(i)h$ for $h\cong T/2$

$$\dot{\boldsymbol{\omega}}(i)Th\cong\left(\mathbf{a}_c(i)+\mathbf{a}_q(i)\right)/2\,. \tag{5.133}$$

1.5.3.2 Noise Estimator

Noise estimate may be obtained through the Kalman filter procedure, paying attention to a pair of facts.

1) A noise channel must be added to the quaternion equation, which corresponds to assume the angular rate $\boldsymbol{\omega}$ driving the equation is erroneous!
2) The quaternion equation is nonlinear, which asks to implement Kalman filter as an extended Kalman filter, suitable to nonlinear dynamics.

A different way can be pursued, similar to the reference generator, trying to be more adherent to the embedded model (5.126), and (ideally) by subtracting from quaternion $\boldsymbol{q}_b$ the reference quaternion $\underline{\boldsymbol{q}}$, in the same way the reference quaternion $\underline{\boldsymbol{q}}$ was cleaned from the nominal quaternion in (5.89). The important result is that the difference between reference and body quaternion is the tracking error $\underline{\boldsymbol{e}}_q$ to be used in the control law

$$\underline{\boldsymbol{q}}=\boldsymbol{q}_b\otimes\underline{\boldsymbol{e}}_b\,. \tag{5.134}$$

Remarks. As in the reference generator, the state predictor is implemented in the nonlinear form (5.126). Linearization is only conceptual for designing the noise estimator.

Assuming a small model error $\delta\boldsymbol{q}_b$ in (5.126), the Euler angle vector $\delta\boldsymbol{\theta}_b$ can be extracted as usual

$$\delta \boldsymbol{q}_b = \delta q_{b0} \begin{bmatrix} 1 \\ \delta \boldsymbol{\theta}_b / 2 \end{bmatrix}. \tag{5.135}$$

The dynamic noise estimator, component-wise and in z-transform notations, is the same as in (5.115)

$$\mathbf{w}(z) = \left(\begin{bmatrix} l_\omega \\ 0 \\ 0 \end{bmatrix} + \frac{1}{z-1+\beta} \begin{bmatrix} m_\omega \\ m_a \\ m_s \end{bmatrix} \right) \delta\theta_b(z) = \mathbf{L}(z)\delta\theta_b(z). \tag{5.136}$$

Less notations the same expressions apply to gain computation and transfer functions.

Figure 11 shows simulated (‘true’) angular accelerations due to gravity gradient and drag torques, and the predicted components. The pitch and yaw components track the ‘true’ profiles (dashed) free of noise. This has been obtained through very slow closed-loop eigenvalue to abate the start tracker noise effect. Slow eigenvalues impose a long transient as it can be seen for the yaw component. The roll component which is close to zero has a significant transient because of an initial error in the attitude and shows irregularities due to star tracker noise. The results show star tracker is only capable of tracking very slow disturbance components. faster components should be predicted by other sensors, like gyroscopes or accelerometers.

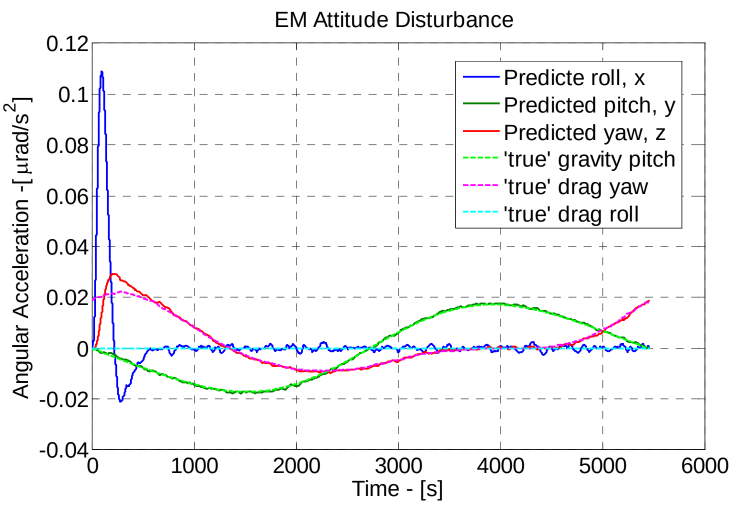

Figure 11. ‘True’ and predicted acceleration disturbance.

1.6 All propulsion drag-free and attitude control

1.6.1 Concept and aims

A pair of goals are aimed to

3) to keep satellite body axes aligned to the local orbit frame (LORF),
4) to zero all accelerations (gravitational and not) below a spectral density bound.

1.6.2 Architecture- attitude control

Figure 8 shows the essential architecture of an attitude control aiming at LORF tracking. The architecture follows the Embedded Model Control

5) The core is the DT Embedded Model (EM) relating command and disturbance to model output to be compared to measurements; a pair of EM are shown: the 'reference' updating reference state $\underline{\mathbf{x}}(i+1)$, the 'actual' providing the one-step prediction of the state $\hat{\mathbf{x}}(i+1)$ in charge of tracking $\underline{\mathbf{x}}(i+1)$. The reference EM is only driven by a 'noise' vector, $\overline{\mathbf{w}}_O(i)$, as it describes 'nature', say the frame attached to the spacecraft orbit. The 'actual' EM is instead driven by thruster command $\mathbf{u}_t(i)$ and 'noise' $\overline{\mathbf{w}}_q(i)$.
6) The spacecraft-to-EM interface is subdivided into the 'reference generator' in charge of estimating the driving noise $\overline{\mathbf{w}}_O(i)$ from GPS measurements, and the measurement law in charge of estimating the noise $\overline{\mathbf{w}}_q(i)$. Source of noise estimation is the model error, here $\overline{\boldsymbol{e}}_q$ and $\overline{\boldsymbol{e}}_O$, generically defined as the difference between measurements and model output, which in this case has to be implemented through quaternion multiplication, for instance as

$$\begin{aligned}\overline{\boldsymbol{e}}_q(i)&=\hat{\boldsymbol{q}}^*(i)\otimes\boldsymbol{y}_q(i)\\ \overline{\boldsymbol{e}}_O(i)&=\hat{\boldsymbol{q}}_O^*(i)\otimes\boldsymbol{y}_O(i)\end{aligned}. \tag{5.137}$$

   The measurement entering the model error requires a treatment to make it comparable to model output, which is done in the boxes 'spacecraft quaternion measurement' and LORF quaternion measurement'.
7) The EM-to spacecraft interface includes the control law, here the cascade of a first box providing the command torques $\mathbf{M}_t(i)$ and a second box creating the thruster commands. Commands are computed one-step ahead and saved, ready to be dispatched at the onset of the relevant interval.

1.6.3 Attitude prediction

1.6.3.1 Attitude sensors

Besides the reference quaternion prediction, the actual attitude prediction must be implemented out of attitude measurements.

Attitude can be measured by different instruments (see Chapter 3), the most common being

1) Earth sensors, in particular infrared Earth sensors, that determine the spacecraft attitude relative to the Earth,
2) Sun sensors, that are present on almost satellites, determine the direction of the spacecraft-sun vector $\mathbf{s}(t)$, thus allowing measurements of only two attitude angles.
3) Star sensors, in particular solid-state (CCD) star trackers, determine the direction of multiple catalogue stars, and through them the spacecraft inertial quaternion $\boldsymbol{q}(t)$ up to measurement errors.
4) Rate integrating gyros provide inertial incremental rate in body coordinates $\boldsymbol{\omega}(t)\Delta t$ up to some error.

Denote the measured quaternion

$$\boldsymbol{y}_q(t) = \boldsymbol{q}(t) \otimes \boldsymbol{e}(t) \tag{5.138}$$

where $\boldsymbol{e}_q(t)$ is the error quaternion.

1.6.3.2 Predictor

The quaternion predictor is implemented as the reference predictor above starting from the measurements. To this end denote the prediction with $\hat{\boldsymbol{q}}(i)$ and repeat the DT kinematic equation

$$\begin{aligned}
&\hat{\boldsymbol{q}}(i+1) = c(i)\hat{\boldsymbol{q}}(i) + \frac{1}{2}s(i)\hat{\boldsymbol{q}}(i)\otimes\left(\hat{\mathbf{v}}(i) + 2L_0\overline{\mathbf{e}}(i)/\overline{e}(i)\right)\\
&c(i) = \cos\left(\hat{\omega}(i)T/2\right)\\
&s(i) = \frac{\sin\left(\hat{\omega}(i)T/2\right)}{\hat{\omega}(i)T/2}\\
&\hat{\mathbf{v}}(i) = \hat{\boldsymbol{\omega}}(i)T
\end{aligned} \quad . \tag{5.139}$$

where the actual model error is defined by

$$\boldsymbol{y}_q(i) = \hat{\boldsymbol{q}}(i) \otimes \overline{\boldsymbol{e}}(i) . \tag{5.140}$$

The dynamic equation is now obtained from Euler equation and must include known disturbance (gravity gradient, gyro torques, ..) and command

$$\begin{aligned}&\hat{\mathbf{v}}(i+1)=\hat{\mathbf{v}}(i)+\hat{\mathbf{a}}(i)+\hat{\mathbf{a}}_d(i)+\mathbf{a}_u(i)+2L_1\overline{\mathbf{e}}(i)/\overline{e}(i),\ \hat{\mathbf{v}}(0)=\hat{\mathbf{v}}_0\\&\hat{\mathbf{a}}(i+1)=\hat{\mathbf{a}}(i)+2L_2\overline{\mathbf{e}}(i)/\overline{e}(i),\ \hat{\mathbf{a}}(0)=\hat{\mathbf{a}}_0\end{aligned}. \tag{5.141}$$

Command acceleration $\mathbf{a}_u(i)$ [rad] if dispatched by a thruster assembly holds

$$\mathbf{a}_u(i)=J^{-1}T^2\mathbf{M}_t(i), \tag{5.142}$$

where $\mathbf{M}_t(i)$ has been defined in Chapter 2. Known disturbance acceleration $\hat{\mathbf{a}}_d(i)$ holds

$$\hat{\mathbf{a}}_d(i)=-J^{-1}\hat{\mathbf{v}}(i)\times J\hat{\mathbf{v}}(i)+\frac{3\mu_E}{\hat{r}_c^5(i)}J^{-1}\hat{\mathbf{r}}_c(i)\times J\hat{\mathbf{r}}_c(i), \tag{5.143}$$

where the gravity gradient term requires the prediction $\hat{\mathbf{r}}_c(i)$ of the CoM position in body coordinates. If not available, the gravity gradient term may be dropped from (5.143) and treated as an unknown acceleration to be accounted for by $\hat{\mathbf{a}}(i)$.

Gain matrices may be designed as in the reference predictor.

1.6.4 Control law

Control law is now direct:

1) to keep attitude quaternion $\hat{\boldsymbol{q}}$ tracking reference $\underline{\boldsymbol{q}}_O$ as well as $\hat{\boldsymbol{\omega}}(i)$ tracking $\underline{\boldsymbol{\omega}}_O(i)$,
2) to reject known and unknown disturbance $\hat{\mathbf{a}}_d(i)$ and $\hat{\mathbf{a}}(i)$, thus leaving the closed-loop control in charge of tracking to act undisturbed,
3) to impose the reference acceleration $\underline{\mathbf{a}}_O(i)$.

The 'actual' tracking errors must be defined

$$\begin{aligned}&\underline{\boldsymbol{q}}_O(i)=\hat{\boldsymbol{q}}(i)\otimes\underline{\boldsymbol{e}}_q(i)\\&\underline{\boldsymbol{e}}_q(i)=\begin{bmatrix}\underline{e}_{q0}\\ \underline{\mathbf{e}}_q\end{bmatrix}\\&\underline{\mathbf{e}}_v(i)=\left(\underline{\boldsymbol{\omega}}_O(i)-\hat{\boldsymbol{\omega}}(i)\right)T\end{aligned}. \tag{5.144}$$

Then the control law holds

$$\mathbf{a}_u(i)=\underline{\mathbf{a}}_O(i)-\hat{\mathbf{a}}_d(i)-\hat{\mathbf{a}}(i)+2K_q\underline{\mathbf{e}}_q/\underline{e}_{q0}+K_v\underline{\mathbf{e}}_v(i), \tag{5.145}$$

where the gain matrices K_q and K_v may be diagonal and their gain selected by fixing the error state matrix

$$\begin{bmatrix}\underline{e}_{qk}\\ \underline{e}_{vk}\end{bmatrix}(i+1)=\begin{bmatrix}1 & 1\\ -k_q & 1-k_v\end{bmatrix}\begin{bmatrix}\underline{e}_{qk}\\ \underline{e}_{vk}\end{bmatrix}(i)+... \tag{5.146}$$

1.6.5 LORF attitude control

1.6.5.1 Embedded model

In this section attitude control will be reduced to a simple form, which applies when attitude angles are kept small, thus after an acquisition phase. The reference frame is assumed to be the LORF and the attitude the body orientation with respect to LORF. The 3-2-1 attitude is assumed as in Chapter 2, and the corresponding quaternion $\delta\boldsymbol{q}(t)$ must be defined as the rotation from LORF to body frame, i.e.

$$\boldsymbol{q}(t) = \boldsymbol{q}_O(t) \otimes \delta\boldsymbol{q}(t) \Rightarrow \delta\boldsymbol{q}(t) = \boldsymbol{q}_O^*(t) \otimes \boldsymbol{q}(t). \tag{5.147}$$

Now assuming small attitude angles

$$\delta\boldsymbol{q}(t) = \begin{bmatrix} \delta q_0 \\ \boldsymbol{\theta}/2 \end{bmatrix} \cong \begin{bmatrix} 1 \\ \varphi/2 \\ \theta/2 \\ \psi/2 \end{bmatrix}. \tag{5.148}$$

The nonlinear kinematic equation comes from Chapter 2, but the rate coordinates are in the LORF (5.72), and the orbit angular rate around the LORF axis $\vec{\mathbf{e}}_h$ must be added, to account for the instantaneous rotation ω_O of the LORF itself

$$\boldsymbol{\omega}(t) = \dot{\varphi}(t)\begin{bmatrix} 1 \\ 0 \\ 0 \end{bmatrix} + \dot{\theta}(t)\begin{bmatrix} 0 \\ \cos\varphi \\ -\sin\varphi \end{bmatrix} + \dot{\psi}(t)\begin{bmatrix} -\sin\theta \\ \sin\varphi\cos\theta \\ \cos\varphi\cos\theta \end{bmatrix} + \begin{bmatrix} 0 \\ \omega_O \\ 0 \end{bmatrix}(t), \tag{5.149}$$

where orbit rate is in general time-varying due to slightly eccentric orbit. Assuming small misalignment between body and LORF, the linear kinematic equation follows, upon definition of the rate deviation $\Delta\omega_y = \omega_y - \omega_O$ wrt to orbital rate

$$\begin{bmatrix} \dot{\varphi} \\ \dot{\theta} \\ \dot{\psi} \end{bmatrix}(t) = \begin{bmatrix} \omega_x \\ \Delta\omega_y \\ \omega_z \end{bmatrix}(t),\ \begin{bmatrix} \varphi \\ \theta \\ \psi \end{bmatrix}(0) = \begin{bmatrix} \varphi_0 \\ \theta_0 \\ \psi_0 \end{bmatrix}. \tag{5.150}$$

Remarks. Equation (5.150) implies LORF and body coordinates can be each other replaced.

In discrete time, upon definition of the time unit T

$$\begin{bmatrix} \varphi \\ \theta \\ \psi \end{bmatrix}(i+1) = \begin{bmatrix} \varphi \\ \theta \\ \psi \end{bmatrix}(i) + \begin{bmatrix} v_x \\ v_y \\ v_z \end{bmatrix}(i), \; \begin{bmatrix} \varphi \\ \theta \\ \psi \end{bmatrix}(0) = \begin{bmatrix} \varphi_0 \\ \theta_0 \\ \psi_0 \end{bmatrix} \\ \begin{bmatrix} v_x \\ v_y \\ v_z \end{bmatrix}(i) = T \begin{bmatrix} \omega_x \\ \Delta\omega_y \\ \omega_z \end{bmatrix}(iT) . \quad (5.151)$$

Passing to Euler equation from Chapter 2

$$\dot{\boldsymbol{\omega}}(t) = -J^{-1}\boldsymbol{\omega}(t) \times J\boldsymbol{\omega}(t) + J^{-1}\mathbf{M}_c(t), \; \boldsymbol{\omega}(0) = \boldsymbol{\omega}_0 , \quad (5.152)$$

one needs to express angular acceleration from (5.150) in body coordinates and to neglect 2nd order terms, which is acceptable as the orbit rate is small $\omega_O \approx 1$ mrad/s

$$\begin{bmatrix} \ddot{\varphi} \\ \ddot{\theta} \\ \ddot{\psi} \end{bmatrix}(t) = \begin{bmatrix} \dot{\omega}_x \\ \dot{\omega}_y - \dot{\omega}_O \\ \dot{\omega}_z \end{bmatrix}(t), \quad (5.153)$$

where $\dot{\omega}_O$ is the orbit acceleration due to non circular orbit. Then

$$\begin{bmatrix} \dot{\omega}_x \\ \Delta\dot{\omega}_y \\ \dot{\omega}_z \end{bmatrix}(t) = -\begin{bmatrix} 0 \\ \dot{\omega}_O \\ 0 \end{bmatrix}(t) + J^{-1}\left(\begin{bmatrix} D_x \\ D_y \\ D_z \end{bmatrix}(t) + \begin{bmatrix} C_x \\ C_y \\ C_z \end{bmatrix}(t) \right), \; \begin{bmatrix} \omega_x \\ \Delta\omega_y \\ \omega_z \end{bmatrix}(0) = \begin{bmatrix} \omega_{x0} \\ \Delta\omega_{y0} \\ \omega_{z0} \end{bmatrix}, \quad (5.154)$$

where the torque vector $\mathbf{M}_c$ has been split into disturbance and command body components D_k and C_k.

Discrete time dynamics is further simplified by treating the orbit acceleration term and the product of inertia terms as disturbance, which amounts to decouple (5.154) into three separate equations

$$\begin{bmatrix} v_x \\ v_y \\ v_z \end{bmatrix}(i+1) = \begin{bmatrix} v_x \\ v_y \\ v_z \end{bmatrix}(i) + \begin{bmatrix} b_x & 0 & 0 \\ 0 & b_y & 0 \\ 0 & 0 & b_z \end{bmatrix}\begin{bmatrix} C_x \\ C_y \\ C_z \end{bmatrix}(i) + \begin{bmatrix} d_x \\ d_y \\ d_z \end{bmatrix}(i), \; \begin{bmatrix} v_x \\ v_y \\ v_z \end{bmatrix}(0) = \begin{bmatrix} v_{x0} \\ v_{y0} \\ v_{z0} \end{bmatrix} \\ b_k = T^2 / J_k \\ d_k(i) = D_k(iT)T^2 / J_k + ... , \quad (5.155)$$

where hyphens stand for orbit acceleration and products of inertia terms. The EM made by (5.151) and (5.155) must be completed by a disturbance model, still decoupled and for simplicity's sake first-order

$$\begin{bmatrix} x_{dx} \\ x_{dy} \\ x_{dz} \end{bmatrix}(i+1) = \begin{bmatrix} x_{dx} \\ x_{dy} \\ x_{dz} \end{bmatrix}(i) + \begin{bmatrix} w_{1x} \\ w_{1y} \\ w_{1z} \end{bmatrix}(i), \quad \begin{bmatrix} x_{dx} \\ x_{dy} \\ x_{dz} \end{bmatrix}(0) = \begin{bmatrix} x_{dx0} \\ x_{dy0} \\ x_{dz0} \end{bmatrix}.$$
$$\begin{bmatrix} d_x \\ d_y \\ d_z \end{bmatrix}(i) = \begin{bmatrix} x_{dx} \\ x_{dy} \\ x_{dz} \end{bmatrix}(i) + \begin{bmatrix} w_{0x} \\ w_{0y} \\ w_{0z} \end{bmatrix}(i) \tag{5.156}$$

It is now possible to design noise estimator and control on a generic single axis possessing the following 3rd order dynamics, where subscripts x, y, z have been dropped and attitude is denoted by θ

$$\begin{bmatrix} \theta \\ v \\ x_d \end{bmatrix}(i+1) = \begin{bmatrix} 1 & 1 & 0 \\ 0 & 1 & 1 \\ 0 & 0 & 1 \end{bmatrix}\begin{bmatrix} \theta \\ v \\ x_d \end{bmatrix}(i) + \begin{bmatrix} 0 & 0 \\ 1 & 0 \\ 0 & 1 \end{bmatrix}\begin{bmatrix} w_0 \\ w_1 \end{bmatrix}(i) + \begin{bmatrix} 0 \\ b \\ 0 \end{bmatrix} C(i), \quad \begin{bmatrix} \theta \\ v \\ x_d \end{bmatrix}(0) = \begin{bmatrix} \theta_0 \\ v_0 \\ x_{d0} \end{bmatrix}. \tag{5.157}$$

Remarks. No noise directly forces attitude in (5.157), which is a key property of (5.157) leading to a particular noise estimator.

1.6.5.2 Attitude measurements

Consider the LORF measured quaternion $\boldsymbol{\mathcal{y}}_O(i)$ and the measured (inertial) attitude quaternion $\boldsymbol{\mathcal{y}}_q(iT)$ in (5.138). Since attitude is here defined wrt to LORF as in (5.147), the attitude quaternion measurement holds

$$\delta\boldsymbol{\mathcal{y}}_q(t) = \boldsymbol{\mathcal{y}}_O^*(t) \otimes \boldsymbol{\mathcal{y}}_q(t) = \begin{bmatrix} \delta y_{q0} \\ \delta \mathbf{y}_q \end{bmatrix}, \tag{5.158}$$

and assuming small attitude as in (5.148) and accounting for measurements errors

$$\delta \mathbf{y}_q(i) = \frac{\delta y_{q0}}{2}\left(\boldsymbol{\theta}(i) + \mathbf{e}_q(i)\right), \tag{5.159}$$

and in scalar form

$$\delta y_q(i) = \frac{\delta y_{q0}}{2}\left(\theta(i) + e_q(i)\right) = \frac{\delta y_{q0}}{2}\left(y_m(i) + e_q(i)\right), \tag{5.160}$$

where e_q is the model error including also measurement errors and $y_m = \theta$ is the EM output signal.

Remarks. In this simple control framework, the reference generator yields the LORF measurement or a prediction, which through (5.158) disappears into the attitude measurement. The resulting control problem is therefore zero-tracking, as the measurement must be kept to zero.

1.6.5.3 Control law

Control law is very simple since aims to keep zero attitude and therefore zero rate and zero acceleration, where the latter is obtained by rejecting disturbance:

$$C(i) = -\left(k_\theta \theta(i) + k_v v(i) + x_d(i)\right)/b\,. \tag{5.161}$$

Remarks. No reference (open-loop) command is included in (5.161).

Gain design is obtained by fixing the eigenvalues of the closed-loop controllable dynamics

$$\begin{aligned} &\det\left(\lambda I - \begin{bmatrix} 1 & 1 \\ -k_\theta & 1-k_v \end{bmatrix}\right) = \gamma^2 + \gamma k_v + k_\theta \\ &\lambda - 1 = \gamma \end{aligned}. \tag{5.162}$$

Then fixing two eigenvalues

$$\Lambda_c = \left\{\lambda_{c0} = 1 - \gamma_{c0}, \lambda_{c1}\right\} \tag{5.163}$$

it results

$$\begin{aligned} k_v &= \gamma_{c0} + \gamma_{c1} \\ k_\theta &= \gamma_{c0}\gamma_{c1} \end{aligned}. \tag{5.164}$$

State variables in (5.161) must be replaced by prediction provided by EM and noise estimator.

1.6.5.4 Noise estimator

It is rather complex as only two noise channels are available in (5.157), ahead of three state variables. To this end a 1st order dynamic feedback must be used to ensure stability while keeping only two noise channels. The resulting state equation is as follows

$$\begin{aligned} &\begin{bmatrix} \hat{\theta} \\ \hat{v} \\ \hat{x}_d \\ q \end{bmatrix}(i+1) = \begin{bmatrix} 1 & 1 & 0 & 0 \\ -l_0 & 1 & 1 & m_0 \\ 0 & 0 & 1 & m_1 \\ -1 & 0 & 0 & 1-\beta \end{bmatrix} \begin{bmatrix} \hat{\theta} \\ \hat{v} \\ \hat{x}_d \\ q \end{bmatrix}(i) + \begin{bmatrix} 0 \\ l_0 \\ 0 \\ 1 \end{bmatrix} \frac{2}{\delta y_{q0}} \delta y_q(i) + \begin{bmatrix} 0 \\ b \\ 0 \\ 0 \end{bmatrix} C(i) \\ &\hat{y}_m(i) = \begin{bmatrix} 1 & 0 & 0 & 0 \end{bmatrix} \begin{bmatrix} \hat{\theta} \\ \hat{v} \\ \hat{x}_d \\ q \end{bmatrix}(i),\ \begin{bmatrix} \hat{\theta} \\ \hat{v} \\ \hat{x}_d \\ q \end{bmatrix}(0) = \begin{bmatrix} \hat{\theta}_0 \\ \hat{v}_0 \\ \hat{x}_{d0} \\ q_0 \end{bmatrix} \end{aligned}, \tag{5.165}$$

where the dynamic feedback state variable is denoted with q and the DT pole by β. The reader is suggested to draw the block-diagram.

Remarks. No forcing function has been added to the first equation in (5.165) for keeping it noise–free.

The four gains to be designed, including β, are related to eigenvalues by the characteristic polynomial

$$\begin{aligned}&\det\begin{bmatrix}\gamma & -1 & 0 & 0\\ l_0 & \gamma & -1 & -m_0\\ 0 & 0 & \gamma & -m_1\\ 1 & 0 & 0 & \gamma+\beta\end{bmatrix} = \gamma^4+\beta\gamma^3+l_0\gamma^2+m_0\gamma+m_1\\ &\gamma=\lambda-1\end{aligned}. \quad (5.166)$$

Thus fixing four eigenvalues $\Lambda_m=\{\lambda_{m0}=1-\gamma_{m0},...,\lambda_{m3}\}$ the following equations derive

$$\begin{aligned}&\beta=\sum_{k=0}^{3}\gamma_{mk}\\ &l_0=\gamma_{m0}\prod_{k=1}^{3}\gamma_{mk}+\gamma_{m1}\left(\gamma_{m2}+\gamma_{m3}\right)+\gamma_{m2}\gamma_{m3}\\ &m_0=\prod_{k=0}^{2}\gamma_{mk}+\prod_{k=1}^{3}\gamma_{mk}+\prod_{k=0,\neq 1}^{3}\gamma_{mk}+\prod_{k=0,\neq 2}^{3}\gamma_{mk}\\ &m_1=\prod_{k=0}^{3}\gamma_{mk}\end{aligned}. \quad (5.167)$$

1.6.5.5 Eigenvalue design with limited thrust

Consider equation (5.161) and introduce a bound to the command torque through an arm a due to thruster application point and max thrust $u_{t,\max}$:

$$k_\theta\left|\theta(i)\right|+k_v\left|v(i)\right|+\left|x_d(i)\right|\le abu_{t,\max}=aT^2u_{t,\max}/J. \quad (5.168)$$

Assuming equal control eigenvalues γ_c in (5.163), (5.168) becomes

$$\gamma_c^2\left|\theta(i)\right|+2\gamma_c\left|v(i)\right|+\left|x_d(i)\right|\le aT^2u_{t,\max}/J. \quad (5.169)$$

Now assume a disturbance bound $\left|x_d(i)\right|\le D_{\max}T^2/J$, an attitude bound $\theta_{\max}$ and the residual attitude to be dominated by 1st order harmonics

$$\left|\theta(i)\right|\le\theta_{\max}\left|\sin\omega_o iT\right|\Rightarrow\left|v(i)\right|\le\omega_oT\theta_{\max}\left|\cos\omega_o iT\right|. \quad (5.170)$$

Then (5.169) becomes

$$\begin{aligned}&\gamma_c^2\theta_{\max}+2\gamma_c\omega_OT\theta_{\max}+D_{\max}T^2/J\le aT^2u_{t,\max}/J\Rightarrow\\ &\gamma_c^2+2\gamma_c\omega_OT-\frac{au_{t,\max}-D_{\max}}{\theta_{\max}J}T^2\le 0\\ &\gamma_c^2+2\gamma_c\alpha-\delta^2\le 0\end{aligned}, \quad (5.171)$$

where δ^2 is the positive fractional margin left by thrust and disturbance bounds to zero tracking. Solving the 2nd order equation

$$-\sqrt{\alpha^2+\delta^2} \le \gamma_c + \alpha \le \sqrt{\alpha^2+\delta^2} \, , \tag{5.172}$$

which reduces to

$$0 < 2\pi f_c T = \gamma_c \le \sqrt{\alpha^2+\delta^2} - \alpha \, , \tag{5.173}$$

to guarantee stability as $\lambda_c = 1-\gamma_c$. Inequality (5.173) shows that higher residual attitude $\theta_{\max}$ and smaller margin δ impose a narrower bandwidth f_c; in the limit $\delta \to 0$, only disturbance rejection would be permitted.

Remarks. The above treatment assumes independency between closed-loop attitude, control gain and disturbance which is not true. Thus the above inequality should be revised in this sense.

Example 1. Fixing $T = 1$ s, $a = 0.5$ m, $J = 2500$ kgm^2, $u_{t,\max} = 1$ mN, $D_{\max} = 0.25$ mNm, $\theta_{\max} = 10^{-4}$ rad it follows

$$\alpha = \omega_O T = 10^{-3},\ \delta^2 = 10^{-3} >> \alpha^2 \Rightarrow \gamma_c \cong \delta \cong 0.033 \, . \tag{5.174}$$

Remarks. In (5.170) prediction errors affecting the control law have been neglected. They should be negligible with respect to bounds assigned to attitude, rate and disturbance.

Passing to account closed-loop interconnections, the residual attitude equation should be written amounting to

$$\begin{bmatrix} \theta \\ v \end{bmatrix}(i+1) = \begin{bmatrix} 1 & 1 \\ -k_\theta & 1-k_v \end{bmatrix}\begin{bmatrix} \theta \\ v \end{bmatrix}(i) + \begin{bmatrix} 0 \\ w_0 + e_d \end{bmatrix}(i),\ \begin{bmatrix} \theta \\ v \end{bmatrix}(i) \, . \tag{5.175}$$

Consider the average low-frequency asymptote $i \to \infty$ under assumption of asymptotic stability

$$\begin{aligned} & 0 = \begin{bmatrix} 0 & 1 \\ -k_\theta & 0-k_v \end{bmatrix}\begin{bmatrix} \underline{\theta} \\ \underline{v} \end{bmatrix}(i) + \begin{bmatrix} 0 \\ \underline{w}_0 + \underline{e}_d \end{bmatrix}(i) \Rightarrow \begin{bmatrix} \underline{\theta} \\ \underline{v} \end{bmatrix}(i) = 0 \\ & \underline{\theta} = \lim_{i\to\infty} \frac{1}{i-j>0} \sum\nolimits_{k=j}^{i} \theta(k) \end{aligned} \, , \tag{5.176}$$

since the noise is zero-mean and the disturbance error should be zero because of EM. Thus the closed-loop error is dominated by transient components (high-frequency) of length comparable to time constant $\tau_c = 1/\gamma_c$. Here noise variance σ_{w0}^2 must be used and short term average $\underline{e}_{d\infty}$ for the residual disturbance. Then just considering the first transient in (5.175)

$$\begin{aligned} \theta(i) &\cong \theta_0 + v_0 i + \sigma_{w0}\sqrt{i^3/3} + \underline{e}_{d\infty} i^2/2 \\ v(i) &\cong v_0 + \sigma_{w0}\sqrt{i} + \underline{e}_{d\infty} i \end{aligned}, \tag{5.177}$$

which at time $i = 1/\gamma_c$ provides

$$\gamma_c^2 \left|\theta(\tau_c)\right| + 2\gamma_c \left|v(\tau_c)\right| \cong \left|\theta_0\right|\gamma_c^2 + 3\left|v_0\right|\gamma_c + \sigma_{w0}\sqrt{\gamma_c}\left(1+1/\sqrt{3}\right) + \left|\underline{e}_{d\infty}\right| 5/2. \tag{5.178}$$

Replacing (5.178) in (5.169) an equation similar to (5.171) is obtained

$$\begin{aligned} &\gamma_c^2 + 3\gamma_c\alpha_\infty - \delta_\infty^2(\gamma_c) \le 0 \\ &\alpha_\infty = \frac{\left|v_0\right|}{\left|\theta_0\right|},\ \delta_\infty^2(\gamma_c) = \left(\frac{au_{t,\max} - D_{\max}}{J} T^2 - \sigma_{w0}\sqrt{\gamma_c}\left(1+1/\sqrt{3}\right)\right)/\left|\theta_0\right| \end{aligned}, \tag{5.179}$$

where residual disturbance terms has been dropped being covered by $D_{\max}$. Solution must be iterated starting by assuming $\gamma_c \le 1$ and can be written as

$$0 < 2\pi f_c T = \gamma_c \le \sqrt{9\alpha_\infty^2/4 + \delta_\infty^2(\gamma_c)} - 3\alpha_\infty/2, \tag{5.180}$$

being of the same type as (5.173), but more conservative if $\left|\theta_0\right| > \theta_{\max}$.

2 References

[1] E. D. Kaplan and C. J. Hegarty eds Understanding GPS. Principles and applications. Artech House, Boston, 2006.

[2] G. F. Franklin, J. D. Powell and M. L. Workman Digital control of dynamic systems, Addison-Wesley, Reading (MA), 1990.

[3] D. T. Greenwood *Principles of dynamics,* Prentice-Hall, Englewood Cliffs, 1965.

[4] J. R. Wertz *Spacecraft attitude determination and control,* D. Reidel Pu. Co. , Dordrecht, 1978

[5] B. Wie *Space vehicle dynamics and control,* AIAA Education Series, AIAA inc, Reston, 1988.

[6] M. J. Sidi *Spacecraft dynamics and control. A practical engineering approach.* Cambridge Univ. Press, 1997.

[7] P. C. Hughes, Peter C., *Spacecraft Attitude Dynamics.* New York, Dover Publications, Inc, 2004.

[8] M. H. Kaplan, *Modern Spacecraft Dynamics & Control.* New York : John Wiley & Sons, 1976.

[9] E. Canuto, *Controlli automatici. Parte II. Controllo digitale,* Celid, Torino, 2002.

[10] ESTEC "ESA pointing error handbook", Doc. EHB.DGP.REP.002, 19 February, 1993, Issue 1.